

**Electrical Characterization of Sulfonated Poly(Styrene-Isobutylene-Styrene) Triblock
Copolymer Thin Films**

By

Martha Ligia Rozo Medina

A thesis submitted in partial fulfillment of the requirements for the degree of

MASTER IN SCIENCES

in

CHEMICAL ENGINEERING

UNIVERSITY OF PUERTO RICO

MAYAGÜEZ CAMPUS

May, 2015

Approved by

Agnes M. Padovani, PhD
President, Graduate Committee

Date

María Curet Arana, PhD
Member, Graduate Committee

Date

David Suleiman, PhD
Member, Graduate Committee

Date

Luis Montejo, PhD
Representative of Graduate Studies

Date

Aldo Acevedo Rullán
Chairperson of the Department

Date

ABSTRACT

Polymers are a fundamental part of electronic systems and are widely used due to their low cost, ease of processing, and their wide range of mechanical and electrical properties. They have traditionally been used as passive components such as insulators and coatings, but more recent applications also include sensors, batteries, and membranes for low-temperature fuel cells. A thorough understanding of the electrical properties is necessary in order to improve their performance and to determine the best design conditions in any given application. The electrical properties of polymeric materials can be characterized through dielectric constant and loss tangent measurements. The first one represents the ability of the material to store potential energy, while the second one represents the losses related to heat dissipation factors. This work is focused on the electrical characterization of sulfonated poly (styrene-isobutylene-styrene) (SIBS) triblock copolymer thin films. More specifically, the dielectric properties of SIBS were evaluated at low frequencies and as a function of critical parameters such as the sulfonation percent and polymer concentration. The sulfonation percent was varied in the range of 0% to 91%, whereas the polymer concentration was studied in the range of 5% to 9%. For the electrical characterization, metal-insulator-metal (MIM) parallel-plate capacitors were fabricated using a combination of physical vapor metal deposition and spin-coating for the polymer films. The electrical measurements were performed using a Network Analyzer that can measure the complex impedance over frequencies in the range of 100 kHz to 1 MHz. The results show that the dielectric constant increases with sulfonation percent and polymer concentration, whereas the loss tangent increase with sulfonation percent, but decrease with polymer concentration. This work provides insights into the correlation of SIBS electrical properties and its chemical structure and morphology.

RESUMEN

Los polímeros son parte fundamental de los sistemas electrónicos y son ampliamente usados debido a su bajo costo, facilidad de procesamiento y amplio rango de propiedades mecánicas y eléctricas. Tradicionalmente han sido empleados como componentes pasivos tales como aislantes y recubrimientos, pero aplicaciones más recientes también incluyen su uso como sensores, baterías y membranas para celdas de combustible a bajas temperaturas

Un amplio conocimiento de las propiedades eléctricas es necesario con el fin de mejorar su rendimiento y determinar las mejores condiciones de diseño para cualquier aplicación específica. Las propiedades eléctricas de los materiales poliméricos pueden ser representadas por la constante dieléctrica y la tangente de las pérdidas eléctricas. La primera representa la habilidad de un material de almacenar energía potencial eléctrica, mientras que la segunda representa las pérdidas relacionadas a efectos disipativos de calor.

Este trabajo está enfocado en la caracterización eléctrica de películas delgadas del copolímero sulfonado de tres bloques poli(estireno-isobutileno-estireno) (SIBS, por sus siglas en inglés). Específicamente, las propiedades eléctricas de SIBS fueron evaluadas a bajas frecuencias en función de parámetros críticos como el porcentaje de sulfonación y la concentración de polímero de las películas. El porcentaje de sulfonación se varió en el rango de 0% a 91%, y la concentración de polímero fue estudiada en el rango de 5 % (p/p) hasta 9% (p/p). Para la caracterización eléctrica se fabricaron condensadores de placas paralelas por medio de las técnicas de deposición de metales y recubrimiento por centrifugado para la fabricación de películas delgadas. Las medidas eléctricas fueron tomadas usando un analizador de redes, el cual provee medidas complejas de impedancia en un rango de 100 kHz a 1MHz. Los resultados indicaron que la constante dieléctrica aumenta con el porcentaje de sulfonación y concentración del polímero. Por su parte, la tangente de las pérdidas aumenta con el porcentaje de sulfonación, pero disminuye con la concentración de polímero. Este trabajo ofrece una comprensión acerca de la correlación de las propiedades eléctricas de SIBS con su estructura química y morfología.

Copyright © 2015
Martha Ligia Rozo Medina.
All rights reserved.

To my beloved family.

ACKNOWLEDGEMENTS

I would like to thank God for all His blessings and to the wonderful people that I have met throughout the completion of my master's degree. To my family for inspiring me achieve my goals, for their trust, love and full support.

Also, I want to express my gratitude to my advisor, Agnes Padovani, for her patience, comprehension, guidance, and advices, not only academic and professional, but for my personal life as well. Her commitment was fundamental to the completion of this work. I extend my gratitude to my graduate committee members, Dr. María Curet, and Dr. David Suleiman for their comments and corrections to this thesis.

I am deeply thankful to Dr. Suleiman and his research group for their invaluable support, especially to Maritza Pérez who had always been so eager to help me.

I express my deepest gratitude to Dr. Rafael Rodríguez for allowing me to use his facilities and for contributing with his knowledge and research experience to the completion of the electrical characterization studies.

Thanks to Dr. Omar Móvil, and the technicians of the Nanomaterials Processing Laboratory, Carlos Rivera and Boris Rentería, for their assistance and advices in the development of the experiments. I am thankful to the undergraduate students who collaborated in this work, especially to Alberto Miranda and Gretchen Quiles for their commitment and contribution.

Also, I am grateful to Dr. Suarez and his research group for sharing good moments with me and making me feel part of their group.

I wish to thank the CREST program (Grant No. HRD-0833112) for their financial support and to the Chemical Engineering Department for this opportunity and for the academic formation that I was able to obtain.

Finally, I wish to thank all my friends, particularly Karen, Ana, Rodinson, Vladimir, and Brian, for all their motivation and for being my family here. And to Misael, for giving me strength when I needed it, and for always being there for me.

Contents

ABSTRACT	ii
RESUMEN	iii
ACKNOWLEDGEMENTS	vi
LIST OF FIGURES	ix
LIST OF TABLES	xi
<i>Chapter 1</i>	1
1.1 INTRODUCTION.....	1
1.2 OBJECTIVES.....	4
<i>Chapter 2</i>	5
2 METHODOLOGY	5
2.1 Materials	5
2.2 EXPERIMENTAL PROCEDURE	5
2.2.1 Sulfonation of SIBS Triblock Copolymer	5
2.2.2 Polymer Solution Preparation.....	6
2.2.3 Fabrication of MIM Capacitors	7
2.3 ELECTRICAL CHARACTERIZATION.....	12
2.4 OPTICAL MICROSCOPY	18
2.5 THICKNESS MEASUREMENTS	20
2.6 POLYMER CHARACTERIZATION.....	20
2.6.1 Chemical Characterization	20
2.6.2 Atomic Force Microscopy	21
2.6.3 Thermo-gravimetric Analysis.....	23
<i>Chapter 3</i>	24
3 RESULTS	24
3.1 CHEMICAL CHARACTERIZATION: FTIR	24
3.2 THERMAL CHARACTERIZATION: TGA	28
3.3 MORPHOLOGICAL CHARACTERIZATION: AFM.....	30

3.4	ELECTRICAL CHARACTERIZATION.....	35
3.4.1	EFFECT OF FREQUENCY.....	35
3.4.2	EFFECT OF SULFONATION.....	39
3.4.3	EFFECT OF POLYMER CONCENTRATION	43
3.4.4	VARIABILITY IN THE ELECTRICAL PROPERTIES	47
3.4.5	REPRODUCIBILITY OF THE ELECTRICAL PROPERTIES	51
<i>Chapter 4</i>	55
4	CONCLUSIONS	55
5	REFERENCES	58

LIST OF FIGURES

Figure 2-1. a) Sputtering system used for electrode deposition. b) Schematic of bottom electrode assembly onto silicon substrate.....	8
Figure 2-2. SIBS thin film deposition via spin-coating: a) spin-coating equipment, b) schematic of fabricated sample.....	8
Figure 2-3. AutoCAD image of the stencil lithography mask used with dimensions: perforation radius: 0.7 mm; distance between perforations: 5 mm; wafer diameter: 76.2 mm.....	10
Figure 2-4. Top electrode deposition using stencil lithography. a) Mask placed prior to metal sputtering. b) Final pattern after removal of mask.	10
Figure 2-5. Experimental setup for the electrical characterization of SIBS thin films.	12
Figure 2-6. Smith Chart. a) Resistance circles. b) Reactance circles. c) Complete Smith Chart.	14
Figure 2-7. Equivalent resistance for fabricated MIM capacitors.	16
Figure 2-8. Optical microscopy images of (a) top electrode at 200x and (b) the scale of 1 mm.....	18
Figure 2-9. Setting the scale for computing the area of the top electrode.....	18
Figure 2-10. Computation of the electrode area using the ImageJ software.	19
Figure 2-11. a) Scratch in the polymer film. b) Placing the sample in the equipment. c) Surface profile to determine the step height of the polymer film.....	20
Figure 2-12. Surface roughness parameters R_a and R_q	22
Figure 3-1. FTIR spectra for: SIBS 0, SIBS 55, SIBS 68, and SIBS 91.	25
Figure 3-2. FTIR spectra of SIBS 55 films at polymer concentrations of 5 wt%, 7 wt% and 9 wt%.....	26
Figure 3-3. FTIR spectra of SIBS 68 at polymer concentrations of 5 wt%, 7 wt% and 9 wt%.....	26
Figure 3-4. FTIR spectra of SIBS 91 films at polymer concentrations of 5 wt%, 7 wt% and 9 wt%.....	27
Figure 3-5. Thermal degradation curves for SIBS 0 and other sulfonated SIBS films.	28
Figure 3-6. a) AFM Topography and b) phase image for SIBS 0.....	30

Figure 3-7. a) AFM Topography and b) phase image for SIBS 55-9%.	31
Figure 3-8. a) AFM Topography and b) phase image for SIBS 68-9%.	31
Figure 3-9. a) AFM Topography and b) phase image for SIBS 91-9%.	31
Figure 3-10. a) Topography and b) phase image for SIBS 68-5.	33
Figure 3-11. a) Topography and b) phase image for SIBS 68-7.	33
Figure 3-12. a) Topography and b) phase image for SIBS 68-9.	34
Figure 3-13. Dielectric constant of SIBS 91-7% as a function of frequency.	36
Figure 3-14. Loss tangent of SIBS 91-7% as a function of frequency.	36
Figure 3-15. Typical polarization mechanisms observed over a range of frequencies. ²³	37
Figure 3-16. Dielectric constant for SIBS thin films as a function of the sulfonation level.	39
Figure 3-17. Loss tangent for SIBS thin films as a function of the sulfonation level.	40
Figure 3-18. Resistivity for SIBS thin films as a function of the sulfonation level.	42
Figure 3-19. Dielectric constant vs. frequency as a function of polymer concentration for SIBS 68.	43
Figure 3-20. Loss tangent vs. frequency as a function of polymer concentration for SIBS 68.	44
Figure 3-21. Dielectric constant vs. frequency for SIBS 91-9%.	45
Figure 3-22. Resistivity as a function of polymer concentration for SIBS 68.	46
Figure 3-23. Surface plot of dielectric constant for SIBS 91-5% at 550 kHz.	48
Figure 3-24. Surface plot of the loss tangent for SIBS 91-5% at 550 kHz.	48
Figure 3-25. Surface plot of the dielectric constant for SIBS 91-7% at 550 kHz.	49
Figure 3-26. Surface plot of the loss tangent for SIBS 91-7% at 550 kHz.	49
Figure 3-27. Surface plot of the dielectric constant for SIBS 91-9% at 550 kHz.	50
Figure 3-28. Surface plot of the loss tangent for SIBS 91-9% at 550 kHz.	50
Figure 3-29. Dielectric constant of replicates of SIBS 91-5% at 100 KHz.	51
Figure 3-30. Dielectric constant for replicates of SIBS 91-5% at 401.5 kHz.	52
Figure 3-31. Dielectric constant for replicates of SIBS 91-7% at 100 kHz.	53
Figure 3-32. Dielectric constant for replicates of SIBS 91-7% at 401.5 kHz.	53

LIST OF TABLES

Table 1. Required weight of polymer for different concentrations.	7
Table 2. Sample combinations of sulfonation-concentration used in this study.	11
Table 3. Parameters to calculate resistance of copper (Cu) and titanium (Ti).	16
Table 4. RMS roughness for SIBS at different sulfonation levels.	32
Table 5. Results of 2t sample test for replicates of SIBS 91-5% and SIBS 91-7%.....	54

1.1 INTRODUCTION

Polymers are essential materials that have contributed to the development of the modern world. They possess a variety of properties that allow their application in a broad range of fields such as agriculture, biomedical, and aerospace, among others. A thorough understanding of these materials properties is therefore necessary in order to improve their performance and determine the best operating conditions for a specific application. Particularly, for electrical, electronic, and electro-mechanical applications, the relative permittivity and loss tangent provide critical design parameter information. The relative permittivity represents the capacity of a material to store electrical energy; the loss tangent represents the dispersive effects or the energy that is lost in the form of heat when an electric field is applied across the material. Therefore, most applications require that the loss tangent be kept as low as possible.¹

Traditionally, polymers have been used as insulating materials for electrical components because of their low dielectric constant, dielectric loss, and high breakdown voltage. These requirements are necessary to ensure the appropriate performance of a device.² For instance, in a dynamic access random memory (DRAM) application, it is required that the intermetal material possesses these characteristics in order to obtain lower delay times and faster storage units.

Some of the most common polymers typically used as insulators include, but are not limited to: polyimides, poly(arylethers), fluoropolymers, heteroaromatic, and hydrocarbon polymers without any polar group. For example, polyimides have dielectric constant values between 2.8 and 3.5. In a particular study, it was observed that the incorporation of fluorine into the polyimide decreases the dielectric constant to values as low as 2.3. However, the presence of fluorine and hydrogen can also lead to corrosion problems, which do not make them suitable for applications in electronics.³

It is important to mention that due to their versatility, polymers can exhibit not only low values of the dielectric constant, but also intermediate and high values by means of the inclusion of ceramic fillers or by chemical modifications.⁴

Terpolymers of vinylidene fluoride, trifluoroethylene, and chlorotrifluoroethylene have been studied for high energy density capacitor applications in medical devices such as external and implanted medical defibrillators. For example, Zhang et al. incorporated chlorotrifluoroethylene (CTFE) into poly(vinylidene fluoride-co-trifluoroethylene) copolymer (PVDF-TrFE) and observed dielectric constant values of nearly 50 at room temperature. This allows the fabrication of smaller capacitors with the same energy density, and contributes to the tendency towards the miniaturization of devices.⁵

Recent work has also taken advantage of the flexibility of polymers to use them as substrates for blendable, rollable, and stretchable electronics. Their good physical and mechanical properties have also been considered for developing polymer matrix composites with high dielectric constants and good processability.⁶ Schumacher *et al.*⁷ studied the effect of adding nano-scaled barium titanate powder to a compounded polyester-styrene matrix. The resulting composite demonstrated an increase in permittivity from 9.2 to 25.0 under room temperature conditions, at a frequency of 1 kHz, and filler loading of 60 wt. %. Therefore, these results suggest that modification of the polymeric matrix and changes in experimental variables such as temperature, rate of measurement (frequency), and moisture level, can have a significant influence in the value of the dielectric constant.⁸

Another interesting class of polymers is the ionomeric block copolymers. They are nanostructured materials composed of two or more monomers covalently linked and phase segregated due the entropic effects among the blocks.⁹ These characteristics allow control of the morphology of the polymer for emerging applications such as Proton Exchange Membranes (PEM).^{10,11} For these polymers, the mechanical and transport properties have been previously studied, but not the electrical properties. The electrical characterization of these polymers could provide insights for future applications in electrical and electronic components. Butkewitsch et al. characterized the relative permittivity and dielectric loss of sulfonated poly(styrene-ethylene/butylenes-styrene) triblock copolymers and analyzed the

effect of moisture content and sulfonation percentage on the samples. The dry material, regardless of the degree of sulfonation, showed values of dielectric constant between 2 and 5. On the other hand, for a polymer sample containing 10% water content and 22% sulfonation level, the dielectric constant increases up to 100,000.⁵ These high values are associated with the presence of sulfonic groups, which tend to absorb great amounts of water, and therefore, induce an increase in the dielectric constant. However, the dissipation factor for this material was about 0.3, which hinders its use in electronic applications because it is above the acceptable operational range by about two orders of magnitude. This implies that the material would produce heat losses that can ultimately affect the efficiency of the device.

In this study, we evaluated the electrical properties of sulfonated poly(styrene-*b*-isobutylene-*b*-styrene) (SIBS) copolymer thin films. Previous studies have demonstrated that this material possesses low temperature flexibility and excellent barrier and mechanical properties, which suggests the following as potential applications: proton exchange membranes, breathable chemical protective clothing, and biomedical implements.¹² Attaining an understanding of the electrical properties of SIBS could therefore diversify the applicability of this material into emerging technologies.

This work is focused on the effect of sulfonation level, polymer concentration, and ac frequency on the relative permittivity and dielectric loss of SIBS thin films in order to contribute to the enhancement of current device design and to propose potential applications for these materials. To accomplish the aims of this project, metal-insulator-metal (MIM) capacitors were fabricated by means of metal sputtering, solvent casting, and spin coating of polymers. Chemical characterization was performed using elemental analysis studies and Fourier Transform Infrared Spectroscopy (FTIR) to determine the level of sulfonic groups in the films. The electrical measurements were performed using a Network Analyzer that gives values of complex impedance over frequencies in the range of 100 kHz to 1 MHz. The values for the dielectric constant and dissipation factor were derived from this data.

1.2 OBJECTIVES

The primary objectives of this investigation are to:

- ❖ Characterize the electrical properties of SIBS triblock copolymer thin films over a range of frequencies by using metal-insulator-metal (MIM) capacitors.
- ❖ Establish structure-property relationships to correlate the electrical properties of SIBS thin films with its chemical, thermal, and morphological properties.

The more specific objectives are to:

- Determine the appropriate processing conditions to fabricate MIM capacitors.
- Study the effect of degree of sulfonation, polymer concentration, and ac frequency on the electrical properties of SIBS.
- Correlate the electrical properties of SIBS thin films with its chemical composition by using the Fourier Transform Infrared Spectroscopy (FTIR) technique.
- Correlate the electrical properties of SIBS thin films with its morphology by using Atomic Force Microscopy (AFM).

2 METHODOLOGY

2.1 Materials

The fabrication of the Metal-Insulator-Metal (MIM) capacitors requires the following reagents and materials: poly(styrene-*b*-isobutylene-*b*-styrene) triblock copolymer (Kaneka® 30 wt.% polystyrene, $M_w = 65,000$ g/mol); toluene (Fisher Scientific, 99.8%); hexyl alcohol (Aldrich Chemical, 98%); methylene chloride (Fisher Scientific, 99.8%); sulfuric acid (Sigma Aldrich, 95-98%); and acetic anhydride (Aldrich Chemical, 99%). For the sputtering process, stainless steel stencils (I-Source Int.) were used and metallic targets of titanium (AJA, 99.999%) and copper (99.995%).

2.2 EXPERIMENTAL PROCEDURE

In this section, the fabrication of MIM capacitors and the characterization techniques used for the SIBS thin films are described.

2.2.1 Sulfonation of SIBS Triblock Copolymer

The sulfonation of the polymer was performed by using the procedure described by Avilés and Suleiman.¹³ First, 30 grams of SIBS were completely dissolved into 200 mL of dichloromethane. Simultaneously, the sulfonating agent was prepared in an ice bath by adding and stirring sequentially, 200 mL of dichloromethane, 13 mL of acetic anhydride, and 7.35 mL of sulfuric acid for ten minutes. The sulfonating agent and the polymer solution were mixed together for 24 hours, followed by the addition of 200 mL of methanol to stop the sulfonation reaction. The solvents were totally evaporated under ambient conditions and then, the polymer was washed with deionized water until the residual water had the same pH as fresh water. Once washed, the polymer was dried at 60°C for 48 hours. Three different degrees of sulfonation were achieved by modifying the amount of sulfonating agent: 55%,

68%, and 91%. These values were selected to evaluate the effect of low, intermediate, and high sulfonation levels on the electrical properties of SIBS thin films.

2.2.2 Polymer Solution Preparation

To achieve the desired concentration, a specific weight of polymer was dissolved for 48 hours in a solution of 85/15 (volume/volume) of toluene and hexyl alcohol, respectively. Toluene is used to dissolve the SIBS polymer and hexyl alcohol is necessary to dissolve the sulfonated groups. For this study, the polymer concentrations selected were 5 wt%, 7 wt%, and 9 wt% because under these conditions, continuous SIBS thin films can be obtained by spin coating. A sample calculation to obtain the required polymer concentration is shown below:

First, the volume of each solvent is calculated based on the ratio 85/15 (toluene/hexyl alcohol). For a total solution of 5 mL, 4.25 mL of toluene and 0.75 mL of hexyl alcohol are required. Then, the total mass of the solvents is obtained using their densities:

$$\text{Toluene: } 4.25 \text{ mL} \times 0.87 \frac{\text{g}}{\text{mL}} = 3.697 \text{ g}$$

$$\text{Hexyl alcohol: } 0.75 \text{ mL} \times 0.82 \frac{\text{g}}{\text{mL}} = 0.615 \text{ g}$$

$$\text{Mass of solvents} = 3.697 \text{ g} + 0.615 \text{ g} = 4.312 \text{ g}$$

Using the following calculation, the weight of the polymer for a specific concentration, X , can be obtained. For example, 5 wt% of polymer concentration will correspond to 95 wt% of solvents.

$$4.312 \text{ g} \rightarrow 0.95$$

$$X \rightarrow 0.05$$

$$X = \frac{0.05 (4.312) \text{ g}}{0.95} = 0.226 \text{ g}$$

Table 1 shows the corresponding polymer weights required for preparing solutions of 5 mL.

Table 1. Required weight of polymer for different concentrations.

Concentration (wt%)	Weight (g)
5	0.226
7	0.324
9	0.426

After weighing the polymer, it is placed in the oven to remove moisture, and finally, the solvents are added and stirred until a homogeneous solution is obtained.

2.2.3 Fabrication of MIM Capacitors

Bottom Electrode Deposition: Sputtering

This process is used to create thin films of a metal or dielectric material onto a surface. To illustrate the process better, the deposition of a thin film onto a silicon wafer will be explained in detail. First, the silicon wafer is placed inside the sputtering chamber and subjected to vacuum lower than 5×10^{-6} Torr. During the process, the substrate is continuously rotated to obtain a homogeneous deposition over the surface. Then, a flow of argon gas is allowed to enter the chamber. The argon atoms are ionized and they get accelerated in the direction of the source material, also known as the target. Collisions eject atoms from the target, which are then deposited onto the substrate forming a thin film. The process operates for a specific amount of time until the desired film thickness is achieved. Finally, the chamber is returned to atmospheric pressure and the sample is removed.

To create the bottom electrode, a titanium-copper-titanium electrode assembly was deposited onto the silicon substrate using the following sputtering conditions:

Ti deposition at 250 W for 10 minutes, followed by Cu deposition at 350 W for 15 minutes, and finally, a second Ti layer is deposited at 250 W for 10 minutes. Figure 2-1 illustrates the sputtering equipment used for this study and the specific electrode assembly fabricated via sputtering.

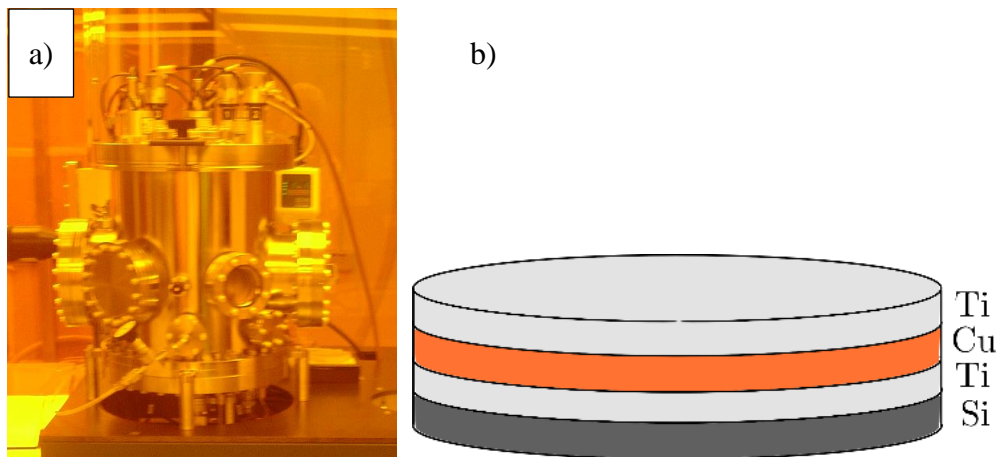


Figure 2-1. a) Sputtering system used for electrode deposition. b) Schematic of bottom electrode assembly onto silicon substrate.

SIBS Thin Film Deposition: Spin Coating

For the SIBS deposition, the polymer solution is poured onto the previously sputtered wafer substrate and placed onto the spin coating equipment (Brewer CE-200), as shown in Figure 2-2a. All samples were spin-coated under the following conditions: pre-spinning velocity of 500 RPM for 10 seconds to spread the polymer over the substrate; followed by spinning at 1000 RPM for 20 seconds to achieve rapid evaporation of the solvent and to obtain continuous thin films. Finally, the sample was soft-baked in a hot plate at 50°C for two minutes and then placed in an oven at 60°C for 48 hours to evaporate the remaining solvent. Figure 2-2b shows an illustration of the electrode-polymer assembly after the deposition of the SIBS thin film.

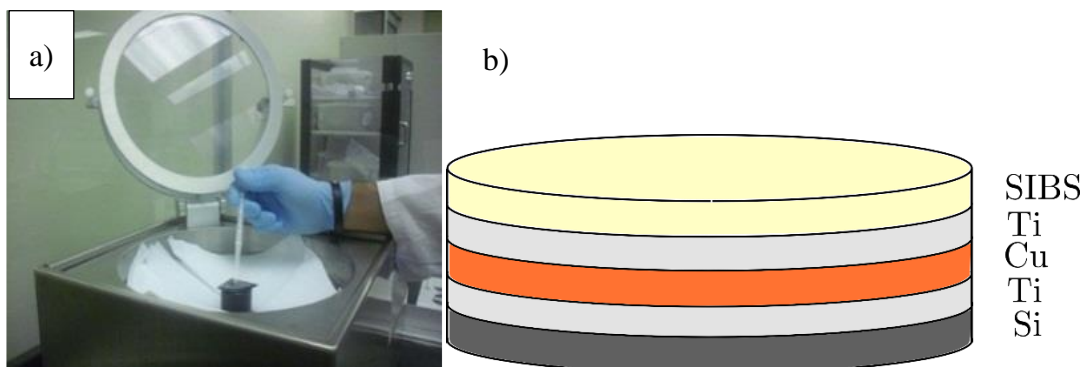


Figure 2-2. SIBS thin film deposition via spin-coating: a) spin-coating equipment, b) schematic of fabricated sample.

Top Electrode Deposition: Sputtering

Traditionally, a photolithography process is used to create patterns onto silicon substrates or metallic films. A photosensitive solution, known as photoresist, is applied over the surface to be patterned. A mask with a design is placed between a UV source and the substrate for patterning and a subsequent step is used to remove the exposed or unexposed photoresist depending on whether it is a positive or negative resist with a solution called developer. Finally, the surface is prepared for additional treatments such as etching or stripping with other chemical solutions. However, some polymers can be contaminated by these chemicals or by UV radiation, which makes them unsuitable for photolithography processing.^{14,15} Such is the case of the sulfonated SIBS polymers.

An alternative technique to create patterns onto these polymers is stencil lithography. This technique uses stencils, based on silicon nitride membranes, which contain nano-scale apertures and are supported on silicon wafers. The stencils are placed on top of the surface to be patterned and put inside the sputtering chamber. The sputtered material passes through the apertures of the stencil to create the desired configuration on the surface.¹⁶ The main challenges of this technique are clogging of the stencils, blurring of the deposited material, and, the stability of the membranes. Takano *et al.* demonstrated the reliability of stencil lithography for sputtering titanium and copper using silicon nitride stencils.¹⁷ The clogging of the stencils was small enough that they could be used several times without cleaning, and the blurring was reduced significantly by decreasing the gap between the stencil and the substrate.

In this investigation, to create the top electrode, a stainless steel stencil with circular apertures (ISource, Inc) was mounted on top of the wafer and placed into the sputtering chamber. The specific mask design used was prepared in AutoCAD, as shown in Figure 2-3. The top titanium-copper-titanium electrode assembly was deposited using the same sputtering conditions as for the bottom electrode. Figure 2-4 shows a schematic of the stencil lithography process used for the deposition of the top electrode.

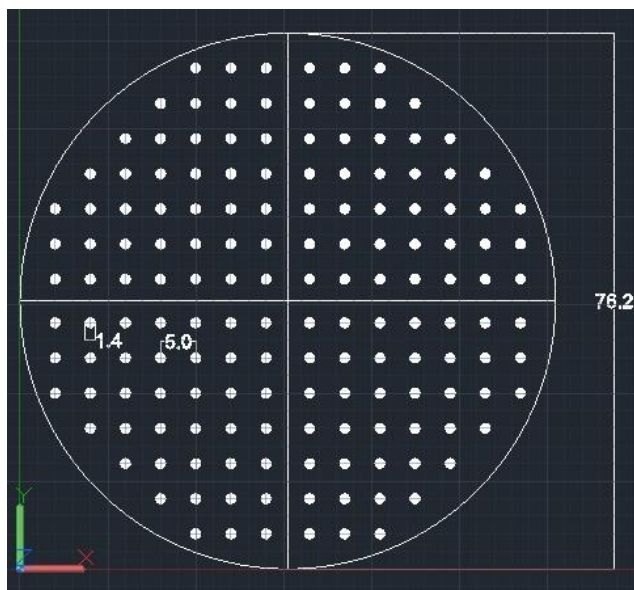


Figure 2-3. AutoCAD image of the stencil lithography mask used with dimensions: perforation radius: 0.7 mm; distance between perforations: 5 mm; wafer diameter: 76.2 mm.

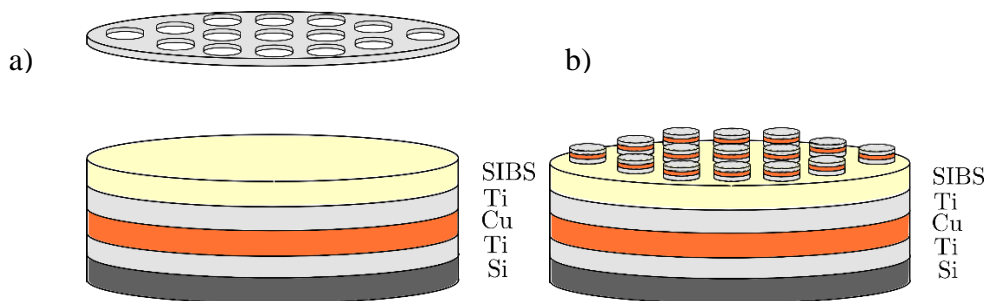


Figure 2-4. Top electrode deposition using stencil lithography. a) Mask placed prior to metal sputtering. b) Final pattern after removal of mask.

Following the sample preparation procedure described before, a series of samples were fabricated by using a combination of polymer concentration and sulfonation percentages. Table 2 lists some of the samples used in this study. The nomenclature used for the samples corresponds to: SIBS XX-Y, where XX is sulfonation level, and Y is polymer concentration.

Table 2. Sample combinations of sulfonation-concentration used in this study.

SAMPLE Name	Sulfonation Percent (%)	Polymer Concentration (wt%)
SIBS 55-5	55	5
SIBS 55-7	55	7
SIBS 55-9	55	9
SIBS 68-5	68	5
SIBS 68-7	68	7
SIBS 68-9	68	9
SIBS 91-5	91	5
SIBS 91-7	91	7
SIBS 91-9	91	9

2.3 ELECTRICAL CHARACTERIZATION

The electrical measurements were performed using a probe station (Signatone 1100 Series) connected to a Network Analyzer (Agilent, E5071C ENA Series 100 kHz-4.5 GHz) that gives values of complex impedance over frequencies in the range of 100 kHz to 1 MHz. The results were recorded both graphically and numerically. Figure 2-5 shows the experimental setup used to characterize the electrical properties of the SIBS thin films.

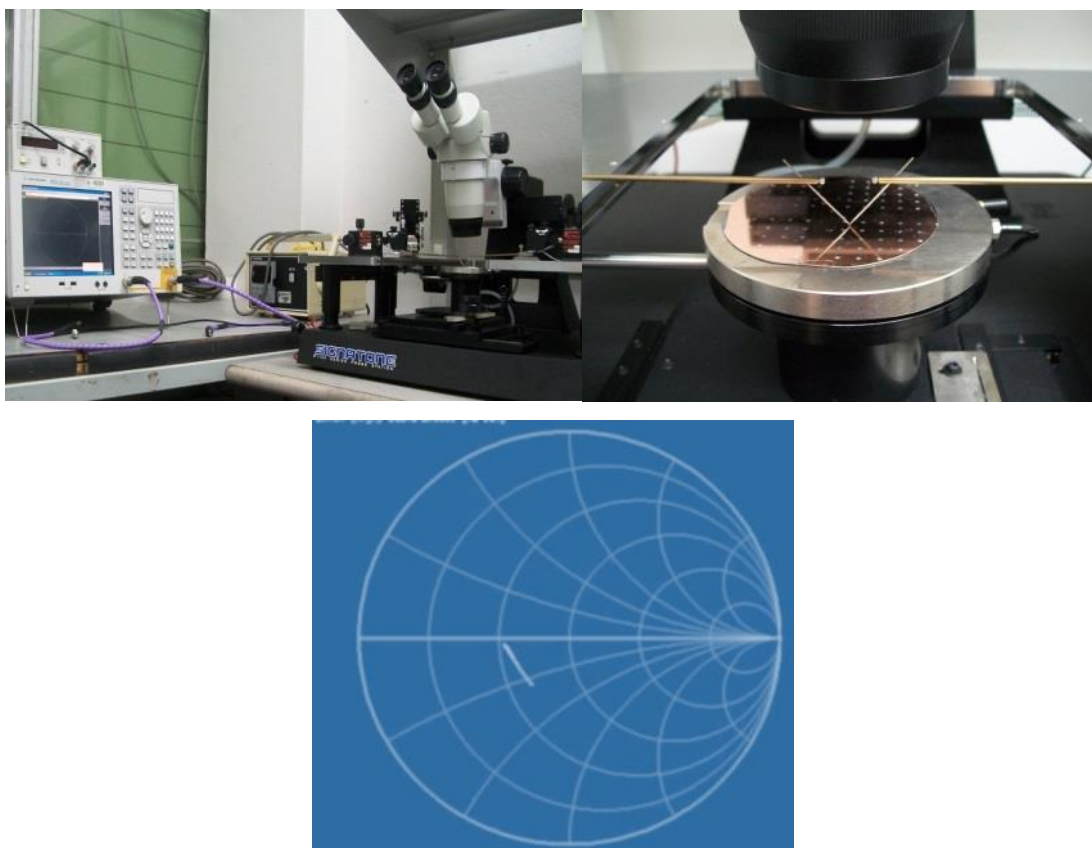


Figure 2-5. Experimental setup for the electrical characterization of SIBS thin films.

The probes are connected to the bottom and top electrodes in the MIM capacitors in order to apply a current through the polymer. The response of the material can be obtained as impedance data, which is readily correlated with the dielectric constant and dissipation factor of the material. A brief explanation of the concepts and equations related to impedance is provided in this section for completeness.

Consider a circuit composed of a resistor, a capacitor, and an inductor in a serial configuration. As current flows through the circuit, it experiences some opposition depending on the element it goes through. For the resistor, the opposition to current is known as resistance and generates a dissipation of energy in the form of heat. In contrast, for capacitors and inductors, the energy is not dissipated, but stored in electric and magnetic fields, respectively. The opposition to current in these latter components is called reactance, which is positive for inductors and negative for capacitors. Impedance represents the total contribution from resistance and reactance, as described in the following equation:

$$Z = R + jX, \quad (\text{Equation 1})$$

where Z is the impedance, R is the resistance, and X is the reactance (in units of Ohms). The reactance, in turn, can be expressed as:

$$X = X_L - X_C, \quad (\text{Equation 2})$$

where X_L is the inductive reactance and X_C is the capacitive reactance.

The complex impedance can be plotted in a Smith Chart, which is comprised of two types of circles: resistance and reactance circles. It is divided by a horizontal line that represents the real part of the impedance (a line of pure resistance). Its values range from zero ($r = 0$) at the left, which also characterizes a short circuit; to infinity ($r = \infty$) at the right, which describes an open circuit. All the values represented in the chart are normalized, that is, result from dividing the actual impedance by a characteristic impedance assigned to the center point of the resistance line. The resistance circles are centered on the horizontal line and are tangent to the right side of the outer circle. For further clarification, schematics of the Smith charts are given in Figure 2-6.

The reactance circles are observed as curved segments since these are circles centered on a vertical line that is perpendicular to the real axis and tangent to the right of the outer circle (Figure 2-6b). Above the center line, the reactance circles have positive values (inductive reactance); and below the center line, negative values (capacitive reactance).

To locate impedance within the Smith Chart, it is necessary to intersect the circle of the specified resistance with the circle of the determined reactance. For example, the impedance $0.5 + j1$ is located by intersecting the circle of 0.5 resistance with the reactance segment of 1 (Figure 2-6c).

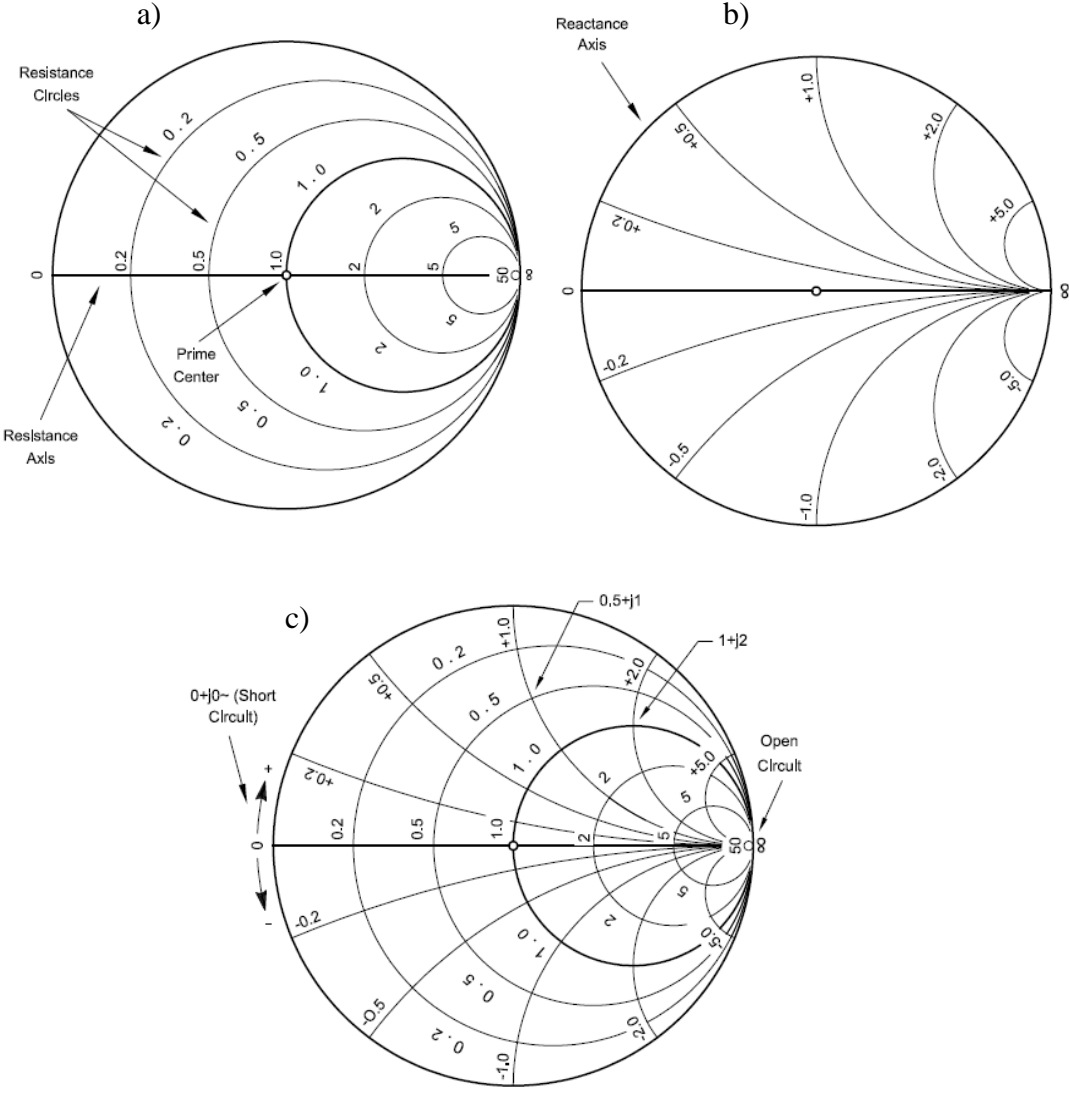


Figure 2-6. Smith Chart. a) Resistance circles. b) Reactance circles. c) Complete Smith Chart.

In this study, according to the assembly of the fabricated capacitors, the only term that needs to be considered is the capacitive reactance, and therefore we have:

$X = -X_C$ [Ω], and

$$X_C = -\frac{1}{2\pi fC} \text{ [\Omega]}, \quad (\text{Equation 3})$$

where f is the frequency (in units of s^{-1}), and C is the capacitance (in units of Farads). After rearrangement for the capacitance:

$$C = -\frac{1}{2\pi fX_C}, \quad (\text{Equation 4})$$

and for parallel plate capacitors, the capacitance can be expressed as:

$$C = \frac{\epsilon_0 \epsilon_r A}{d}, \quad (\text{Equation 5})$$

where ϵ_0 is the vacuum permittivity (8.854×10^{-12} F/m), ϵ_r is the dielectric constant, A is the cross-sectional area (m^2), and d defines the spacing between the parallel plates (m). After some algebraic manipulations, we obtain the desired expression for the dielectric constant:

$$\epsilon_r = \frac{Cd}{\epsilon_0 A}. \quad (\text{Equation 6})$$

Dissipation Factor

The dissipation factor can be obtained from the real part of the impedance. The expression used to calculate it is described in equation 7.

$$\tan \delta = \frac{1}{\rho_{SIBS} \omega \epsilon_r \epsilon_0} \quad (\text{Equation 7})$$

where $\tan \delta$ is the dissipation factor, ρ_{SIBS} is electrical resistivity of the SIBS thin films, and $\omega = 2\pi f$.

Therefore, the resistivity of the polymer needs to be measured. This value can be obtained from the resistance gathered from the network analyzer, the area of the capacitor, and the thickness of the polymer, as expressed by the following equation:

$$R = \frac{\rho l}{A} \rightarrow \rho = \frac{RA}{l}, \quad (\text{Equation 8})$$

where R is the resistance (Ω), ρ is the electrical resistivity ($\Omega \cdot \text{m}$), l is the thickness of the polymer (m), and A is the cross-sectional area of the electrode (m^2).

The assembly of the MIM capacitors represents an equivalent resistance for series resistors, as shown in Figure 2-7.



Figure 2-7. Equivalent resistance for fabricated MIM capacitors.

In turn, the resistance of the metals could be calculated using the information in Table 3.

Table 3. Parameters to calculate resistance of copper (Cu) and titanium (Ti).

Metal	Resistivity(Ωm)	Thickness (m)	Area (m^2)
Copper	1.676×10^{-8}	5.35×10^{-7}	1.46×10^{-6}
Titanium	0.7×10^{-6}	1.124×10^{-7}	1.46×10^{-6}

The resistance of Cu (R_{Cu}) and Ti (R_{Ti}) are found using the following calculations:

$$R_{Cu} = \frac{\rho l}{A} \rightarrow = \frac{1.676 \times 10^{-8} \Omega \text{m} \cdot 5.35 \times 10^{-7} \text{m}}{1.46 \times 10^{-7} \text{m}^2} = 6.183 \times 10^{-8} \Omega,$$

$$R_{Ti} = \frac{\rho l}{A} = \frac{0.7 \times 10^{-7} \Omega \text{m} \cdot 1.124 \times 10^{-7} \text{m}}{1.46 \times 10^{-7} \text{m}^2} = 5.426 \times 10^{-8} \Omega$$

Therefore, the total resistance R_T is given by the following expression:

$$R_T = 4R_{Ti} + 2R_{Cu} + R_{SIBS}$$

where R_{SIBS} is the resistance of the SIBS thin film. Values of resistance gathered from the network analyzer vary in the range from 12 Ω to 25 Ω , and hence, for the smallest value obtained we have:

$$12 \Omega = 2.17 \times 10^{-7} \Omega + 1.23 \times 10^{-8} \Omega + R_{SIBS},$$

$$R_{SIBS} = 11.999 \Omega.$$

As a result, the resistance of the metals can be neglected and the measurement can be approximated to the resistance of the polymer film.

To calculate the area of the electrodes and the thickness of the thin films, optical microscopy and profilometry techniques were used, respectively.

2.4 OPTICAL MICROSCOPY

In order to measure the superficial area of the electrodes, optical microscopy was used. An image of the top electrode is shown in Figure 2-8 at a magnification of 200x. Another image (at the same magnification) with a 1 mm scale was used to measure the area of the electrode. This procedure is performed using the ImageJ software.

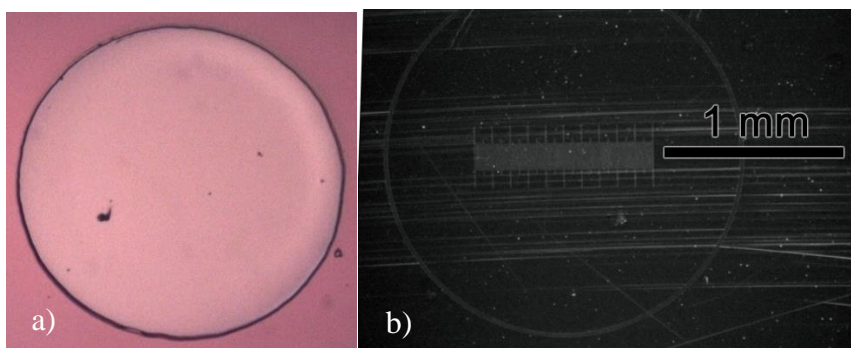


Figure 2-8. Optical microscopy images of (a) top electrode at 200x and (b) the scale of 1 mm.

First, the same resolution of the image with the scale is applied to the image of the top electrode using Adobe Photoshop. Then, the image with the scale is opened in ImageJ and a line is drawn on the bar containing the scale to set an equivalence from pixels to millimeters. Figure 2-9 shows a characteristic ImageJ scaling window.

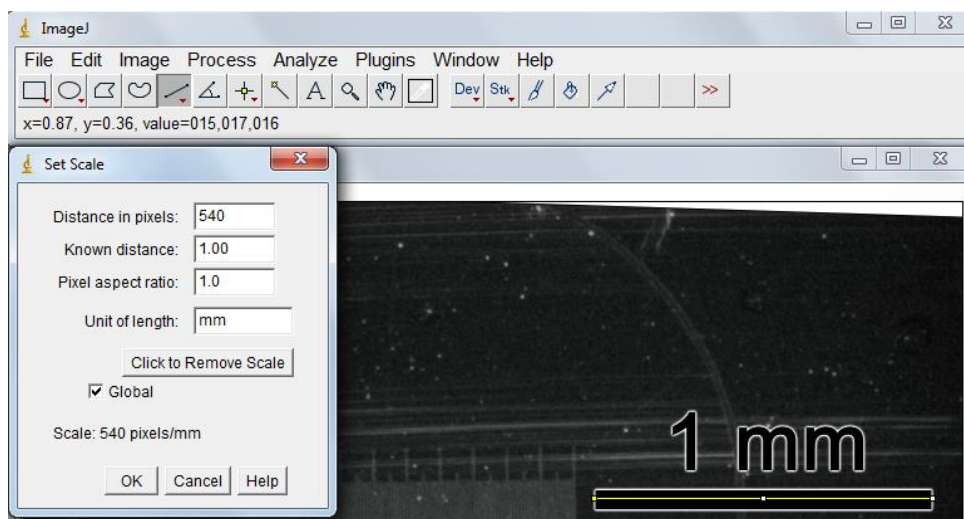


Figure 2-9. Setting the scale for computing the area of the top electrode.

Finally, the image of the electrode is also opened with ImageJ and a circle that fits its contour is drawn. Figure 2-10 shows a schematic of the procedure used to determine the area. The area of this circle represents the area of the electrode, which is calculated by the software and used for the electrical computations.

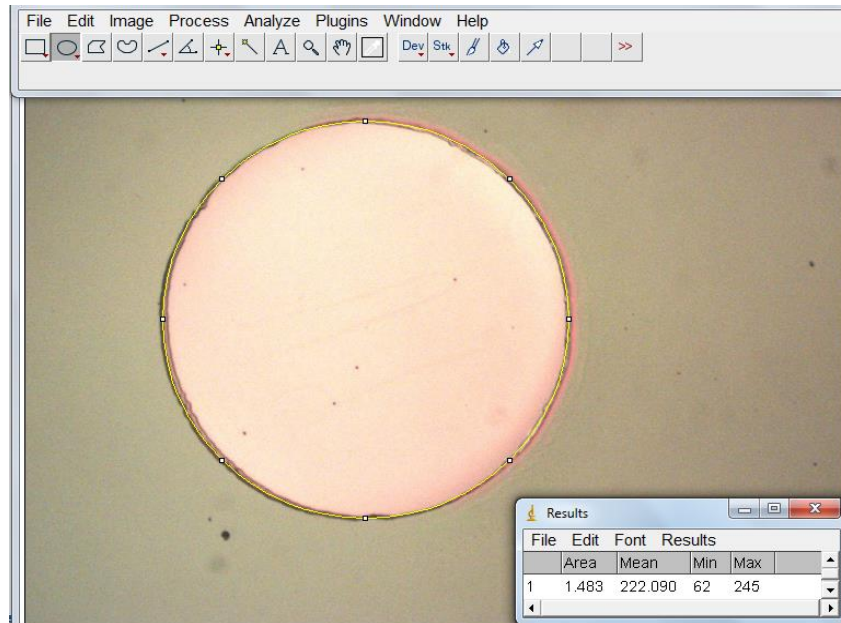


Figure 2-10. Computation of the electrode area using the ImageJ software.

2.5 THICKNESS MEASUREMENTS

The thickness of the polymer films was determined using a Surface Profiler (KLA Tencor, Model: P-6). For these studies, a small scratch is made into the polymer film in an area close to the capacitor and the thickness is measured using a step profile.

A probe scans the surface of the polymer, which is on top of the bottom electrode. The scan process captures the scratch and produces an image with the surface profile, which is then used to estimate the thickness of the polymer film. Figure 2-11 shows the various steps performed for the thickness measurements.

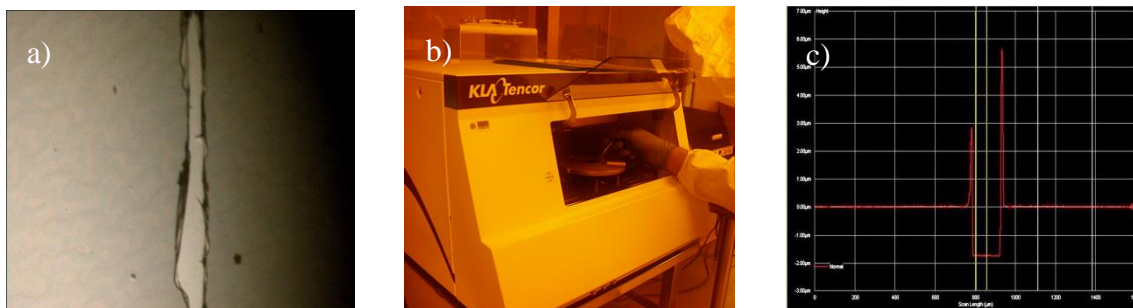


Figure 2-11. a) Scratch in the polymer film. b) Placing the sample in the equipment. c) Surface profile to determine the step height of the polymer film.

2.6 POLYMER CHARACTERIZATION

The samples were characterized using elemental analysis, Fourier Transform Infrared Spectroscopy (FTIR), Thermo-gravimetric Analysis (TGA), and Atomic Force Microscopy (AFM) in order to study the chemical composition, thermal behavior, and morphology, respectively. These results were correlated for further understanding of the electrical properties of the material.

2.6.1 Chemical Characterization

The chemical characterization of the samples was performed using elemental analysis and Fourier Transform Infrared Spectroscopy (FTIR) techniques.

The elemental analysis technique is used to determine the amount of an element in a compound. It consists of the combustion of an organic sample in an atmosphere with excess of oxygen. The resulting gases from the combustion are transported in a high purity helium carrier gas to a chromatographic column, where the analytical species are quantified. For the elemental analysis, the samples were sent to Atlantic Microlab Inc. in Norcross, GA for determination of the percent of carbon, nitrogen, and sulfur. The degree of sulfonation was calculated based upon these results.

Fourier Transform Infrared Spectroscopy is an analytical technique that allows the chemical identification of compounds and substituents. It is based upon the interaction between infrared light and the molecules. When infrared radiation passes through a sample, part of it is absorbed and the other part is transmitted. The resulting spectrum consists of peaks that are related to frequencies of vibration of the atomic bonds, which represent a molecular fingerprint for the sample.¹⁸ In the present work, the FTIR analysis was performed at The Nanomaterial and Processing Laboratory located in room S-314 of the Stefani building. The FTIR (Shimadzu, IRAffinity-1) was used to confirm the presence of the sulfonic groups and as an indirect measurement of the sulfonation level by correlating the intensity of the peaks to the sulfonation level. The SIBS thin films were characterized in ATR mode in the range from 550 to 4000 cm^{-1} using 300 scans and a resolution of 4 cm^{-1} .

2.6.2 Atomic Force Microscopy

Atomic force microscopy (AFM) allows for measuring the surface topography of a material. For this purpose, a cantilever with a short probe scans over a sample and variations in height due to the surface-tip interactions produce an image of the surface. The probe can scan over the surface in direct contact with the sample (contact mode), close to the sample (non-contact mode) or oscillate over the sample (dynamic contact mode).

The morphologies of SIBS thin films at different sulfonation levels and polymer concentrations were studied using an atomic force microscope (Agilent AFM 550) in dynamic contact mode. The topography and phase images of the thin films were obtained with PPP-NCH probes (Keysight Technologies) with a resolution of 256 px.

The surface roughness was calculated for the films in this study in order to obtain a quantitative measurement that could be used for comparison. The Gwyddion software was used for this purpose based on the ASME B46.1 and ISO 4287 standards. Surface roughness is determined by the vertical spacing of a scanned surface from its ideal form. Therefore, for larger spacing the surface is rougher. This parameter is frequently reported as Arithmetic Average Roughness (R_a), and as Root Mean Square Roughness (R_q). The first one is defined as the arithmetic average of all the peaks and valleys of a surface profile with respect to the mean line over the evaluation length. The equation for calculating R_a is:

$$R_a = \frac{1}{N} \sum_{j=1}^N (z_j - \bar{z}) \quad (\text{Equation 9})$$

Where N represents the number of data points over the z evaluated; z is the height of the peak or valley, and j is its position within the evaluation length.

The Root Mean Square Roughness (R_q) is the root mean square average of the height deviations from the mean line within the evaluation length:

$$R_q = \sqrt{\frac{1}{N} \sum_{j=1}^N (z_j - \bar{z})^2} \quad (\text{Equation 10})$$

Figure 2-12 illustrates the parameters described for further clarification.

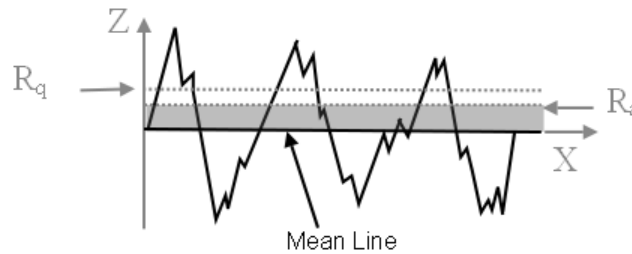


Figure 2-12. Surface roughness parameters R_a and R_q .

2.6.3 Thermo-gravimetric Analysis

Thermogravimetric Analysis (TGA) is a technique used to determine the thermal stability of a material and its degradation characteristics. The technique monitor changes in mass over a range of time and temperature. Each degradation step can be correlated with the degradation of a specific functional group or compound present in the material.

The degradation temperatures, as well as the water content absorbed by the polymer, were evaluated as function of the sulfonation percent in the films. For this study, a METTLER Toledo TGA was used in the range from 25°C to 600°C with a ramp temperature of 5°C/min.

3 RESULTS

3.1 CHEMICAL CHARACTERIZATION: FTIR

For these studies, the FTIR technique was used to characterize SIBS polymer membranes containing 0% (SIBS 0), 68% (SIBS 68), and 91% (SIBS 91) sulfonation percentages in order to confirm the presence of sulfonic groups in the polymer membranes. The software KnowItAll® was used to plot the resulting spectra and identify the characteristic peaks of the samples. Direct comparison of the spectra in Figure 3-1 for the low (55%), intermediate (68%), and highly sulfonated (91%) polymer membranes with respect to the unsulfonated one (0%), shows the presence of new bands at 1033 cm^{-1} and 1152 cm^{-1} . The peak at 1033 cm^{-1} represents the symmetric stretching vibration of the S=O bond (1100 to 1000 cm^{-1}), whereas the peak at 1152 cm^{-1} is characteristic of the asymmetric stretching vibration of the S=O bond (1250 to 1150 cm^{-1}). These results suggest that sulfonic groups (-SO₂OH) were successfully incorporated into the polymer membranes.

Two additional peaks at 1635 cm^{-1} and 3399 cm^{-1} are present in the sulfonated polymer membranes, conversely to the SIBS 0 sample. These peaks correspond to the presence of water and solvents in the membranes. Also, it can be observed that as the sulfonation level increases from 55% to 91%, the intensity of the bands associated with the sulfonic groups increases, which indirectly confirms that the sulfonation level is also increasing.

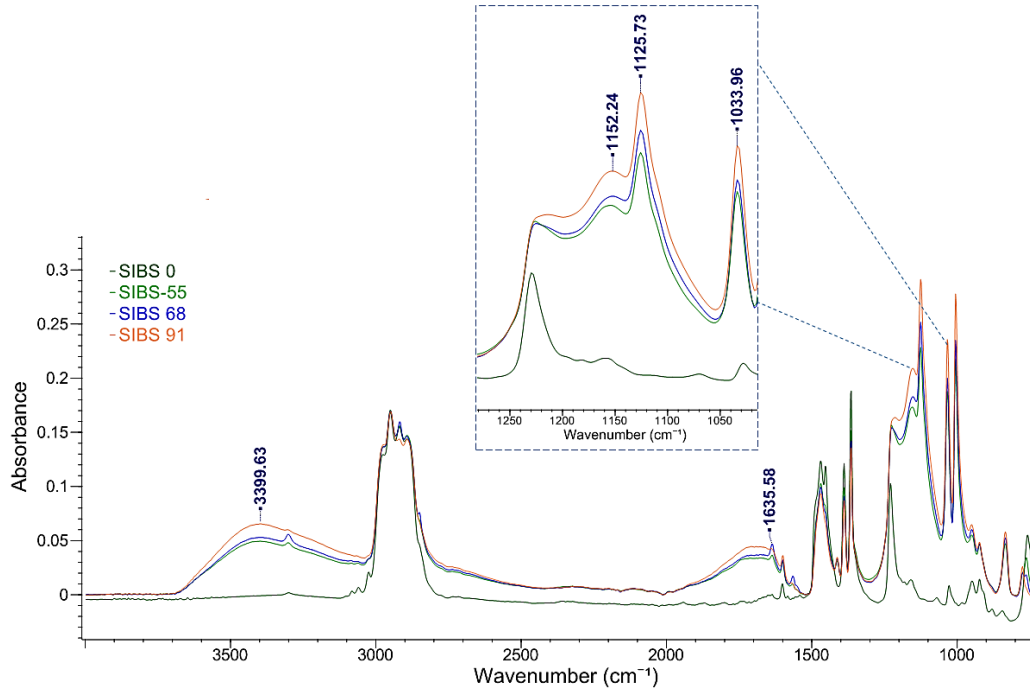


Figure 3-1. FTIR spectra for: SIBS 0, SIBS 55, SIBS 68, and SIBS 91.

Figure 3-2 to Figure 3-4 show the FTIR spectra for SIBS thin films deposited on silicon wafer under the same spin coating conditions that were used to fabricate the MIM capacitors, that is, 10 seconds for pre-spinning at 500 RPM and 30 seconds of spinning at 1000 RPM. The spectra were recorded as a function of the polymer concentration in the films. The specific concentration range studied varied from 5 wt% to 9wt%.

The spectra show that the peaks corresponding to the sulfonic groups are slightly intensified at higher concentrations of the polymer, regardless of the sulfonation level. This occurs because there are more chains entangled to each other within the film, and therefore, more sulfonic groups are present in qualitative agreement with the mentioned figures.

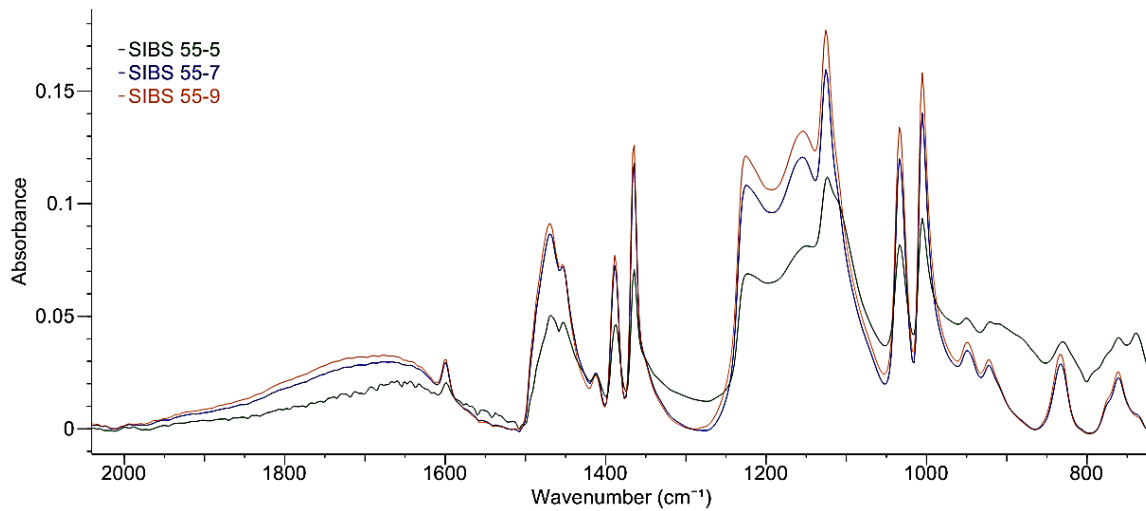


Figure 3-2. FTIR spectra of SIBS 55 films at polymer concentrations of 5 wt%, 7 wt% and 9 wt%.

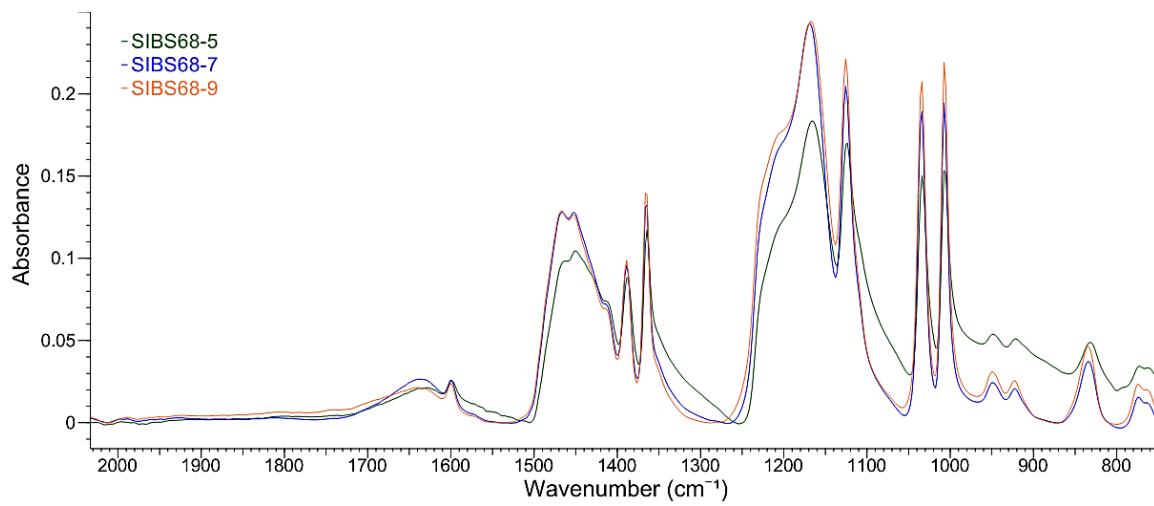


Figure 3-3. FTIR spectra of SIBS 68 at polymer concentrations of 5 wt%, 7 wt% and 9 wt%.

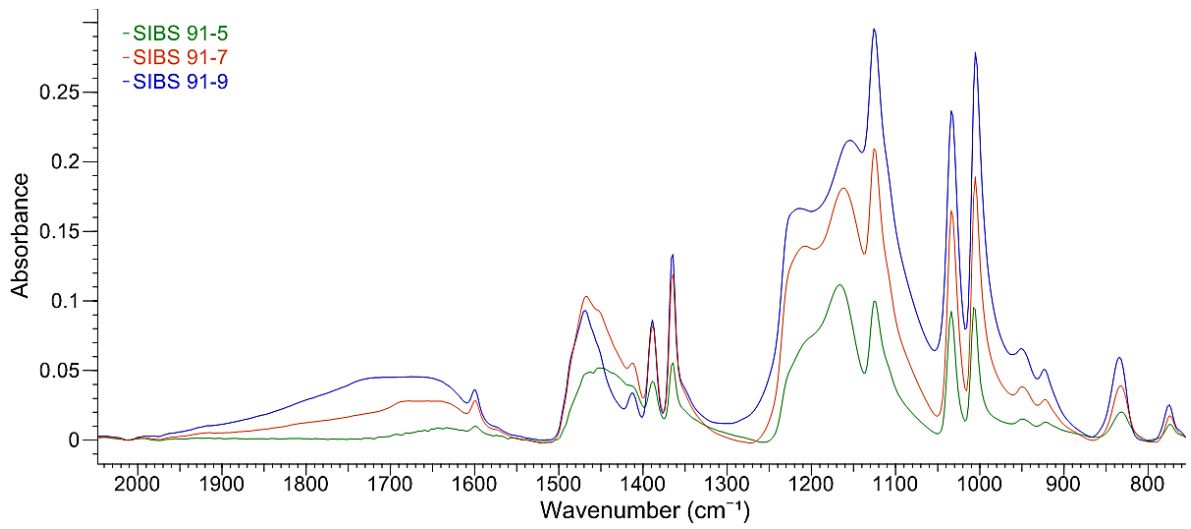


Figure 3-4. FTIR spectra of SIBS 91 films at polymer concentrations of 5 wt%, 7 wt% and 9 wt%.

3.2 THERMAL CHARACTERIZATION: TGA

In this study, the thermogravimetric analysis was used to evaluate the effect of the sulfonation treatment on the thermal stability of the SIBS films, and to determine the degradation mechanisms of the polymer. The curves for the thermal stability of SIBS 0, SIBS 55, SIBS 68, and SIBS 91 are shown in Figure 3-5.

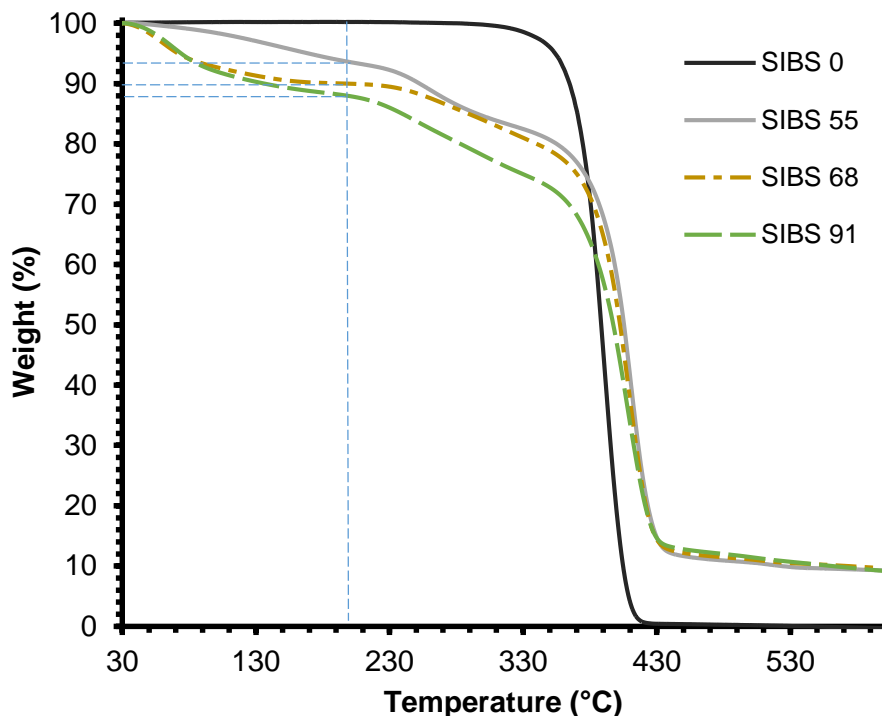


Figure 3-5. Thermal degradation curves for SIBS 0 and other sulfonated SIBS films.

In the case of SIBS 0, the curve shows that there is only one region of weight loss in the range of 330°C to 440°C. This weight loss corresponds to the degradation of both, the poly(styrene) and the poly(isobutylene), which usually are non-differentiable according to other studies.¹² On the other hand, three different regions of weight loss are observed for the sulfonated membranes. The first region of weight loss spans from approximately 30°C to 200°C, and this corresponds to the evaporation of solvents and moisture trapped within the polymer. A detailed analysis of the first degradation region revealed that the weight loss increases with the sulfonation percentage in the films. The percentage of water plus solvents

can be estimated by drawing a vertical line at 200°C and reading the value when this line crosses each corresponding TGA curve (dashed lines in Figure 3-5). For SIBS 55, this percentage is about 6 wt%; for SIBS 68 is 10 wt%, and for SIBS 91 is 13 wt%. These results are somehow expected for films with high concentration of sulfonic groups because of their strong affinity to water. Also, the water uptake increases as the groups become more interconnected. These observations are consistent with prior studies reported of SIBS polymers.^{19,20}

The second weight loss step in the thermal stability curves for the SIBS films corresponds to the decomposition of the sulfonic groups. This degradation is observed in the region between 200°C and 400°C. Other studies with sulfonated polymers have found that the decomposition of the sulfonic groups occurs at similar temperatures to those reported in this work.^{12,21} For example, Suleiman *et. al*,¹² found for SIBS that this degradation occurs at 290°C for SIBS, when the sulfonated groups are detached from the styrene rings.²¹

Finally, the third weight loss step was recorded in the range from 400°C to 460°C, and it can be attributed to the degradation of the polymer backbone, that is, the poly(styrene) (PS) and poly(isobutylene) (PIB) chains. The inflection point for all the curves was $410 \pm 5^\circ\text{C}$. Therefore, this suggests that the degradation temperatures of PS and PIB are quite close, which is again in accordance with prior results reported by Avilés.²⁰

Regarding the ultimate objective of this investigation, which is to characterize the electrical properties of the sulfonated membranes, it is relevant to point out that the thermal characterization revealed a high amount of absorbed water that increased with the degree of sulfonation. Accordingly, this suggests that the electrical properties of the sulfonated polymer membranes will likely be affected by the water content because water is a substance with a high dielectric constant. Similarly, these effects are expected to be more pronounced as the level of sulfonation increases in the polymer films.

Finally, keeping in mind the potential application of these materials into electronic devices, the thermal analysis shows that the operational temperature should be kept below 200°C to avoid polymer degradation issues and/or the detachment of the sulfonic groups.³

3.3 MORPHOLOGICAL CHARACTERIZATION: AFM

Atomic Force Microscopy (AFM) studies were performed to evaluate the changes in morphology as function of sulfonation level and polymer concentration in the films. For this purpose, topography and the corresponding phase images were obtained by using AFM in dynamic contact mode or the most commonly known tapping mode. Surface roughness was measured with the Gwyddion software to obtain a quantitative measurement that could be used to compare the different films.

The effect of sulfonation on morphology was evaluated by comparing the SIBS 0, SIBS 55-9%, SIBS 68-9%, and SIBS 91-9% samples, as illustrated in Figure 3-6 to Figure 3-9. From the topography images, a continuous surface is observed for SIBS 0. However, as the sulfonation level is increased to 55% the surface topography becomes more irregular with small waviness that represents the phase segregation enhanced by the presence of sulfonic groups.²² At 68% the waviness becomes wider and more peaks and valleys are present. For SIBS 91-9%, the topography is similar to the SIBS 68-9% sample, but the amplitude of the peaks and valleys is intensified. These results suggest that the increase in sulfonation level promotes the aggregation of larger ionic domains.

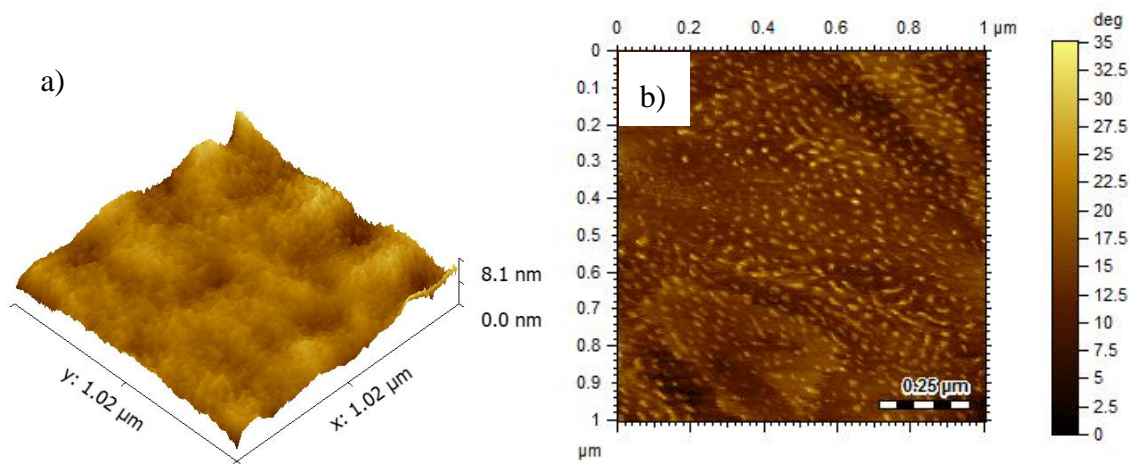


Figure 3-6. a) AFM Topography and b) phase image for SIBS 0.

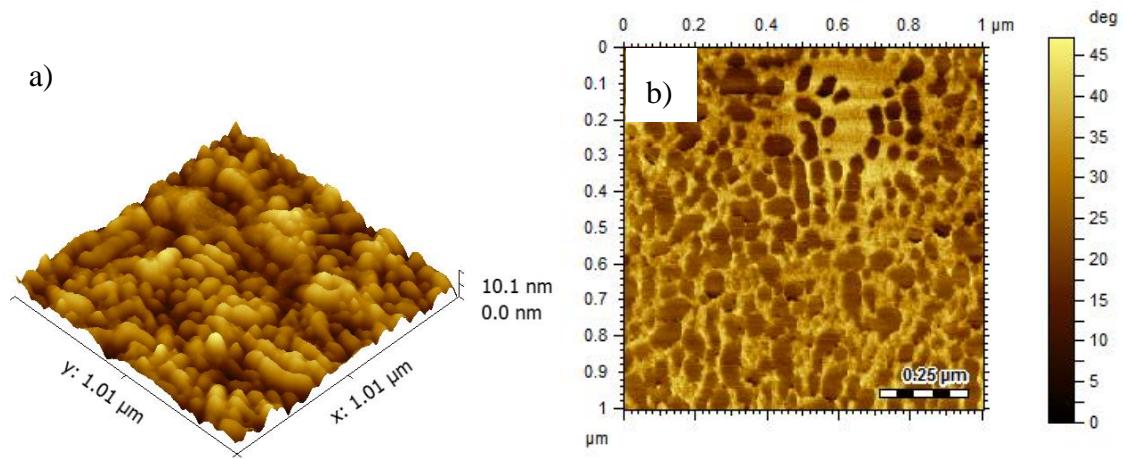


Figure 3-7. a) AFM Topography and b) phase image for SIBS 55-9%.

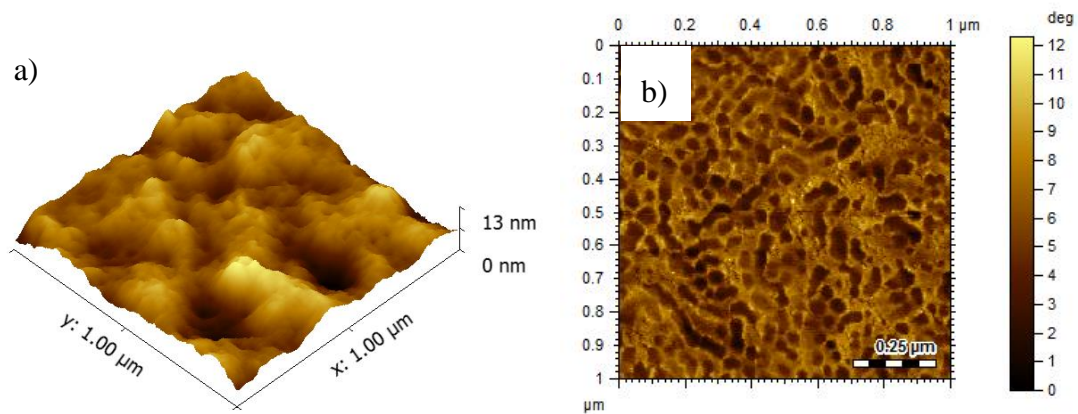


Figure 3-8. a) AFM Topography and b) phase image for SIBS 68-9%.

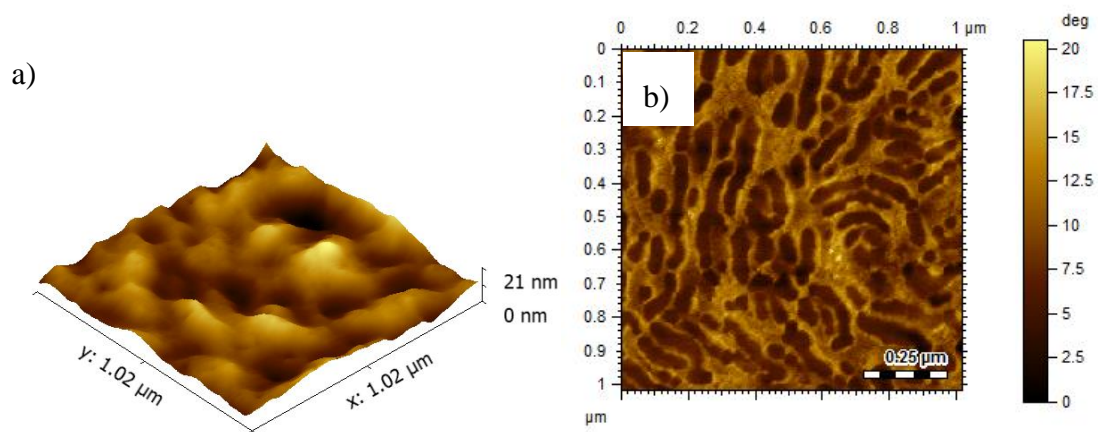


Figure 3-9. a) AFM Topography and b) phase image for SIBS 91-9%.

From the topography data recorded, the surface roughness of the samples was also calculated. The results for the root mean square roughness are shown in Table 4.

Table 4. RMS roughness for SIBS at different sulfonation levels.

Sample	R_q (nm)
SIBS 0	0.619
SIBS 55-9%	1.464
SIBS 68-9%	1.85
SIBS 91-9%	2.99

The roughness varied from 0.619 nm for SIBS 0 to 2.99 nm for SIBS 91-9%, which implies that the surface becomes rougher as the sulfonation level increases.

The phase images also confirm the change in morphology observed in the topography images due to the chemical functionalization of PS with sulfonic groups. Figure 3-6b shows circular domains for SIBS 0 that consist of PS segregated in a PIB matrix. It is interpreted that the circular domains correspond to the top view of a hexagonal packed cylindrical morphology.^{23,24} This morphology is characteristic of PS when it is embedded in an elastomeric matrix such as poly(acrylic acid-b-styrene-b-isobutylene-b-styrene-b-acrylic acid) pentablock copolymer (PAA), as has been previously reported by James *et al.*²⁵

At 55% sulfonation (Figure 3-7b), the phase image shows short cylinders, which suggest the formation of nanochannels as a result of the electrostatic and dipole-dipole interactions between the sulfonic groups. As the sulfonation increases to 68%, the presence of more sulfonic groups promotes additional interactions that lead to more interconnected nanochannels or ionic domains (Figure 3-8b). This tendency is intensified at the highest sulfonation studied (91%) for which larger nanochannels and more continuous non-ionic domains (PIB matrix) are observed (Figure 3-9b).

Similar results were observed when the polymer concentration was varied. Films for SIBS 68 at polymer concentrations of 5 wt%, 7 wt%, and 9 wt% were considered in this study. These results are shown in Figure 3-10 to Figure 3-12. For SIBS 68-5% short cylinders and isolated circular patterns were present. As the polymer concentration is increased to 7 wt%

the cylinders are still short, but become wider and more defined. At the highest concentration, 9 wt%, the cylinders and circles become closer and in some instances, they display a certain degree of interconnection, which is evidenced in the size of the cylinders observed.

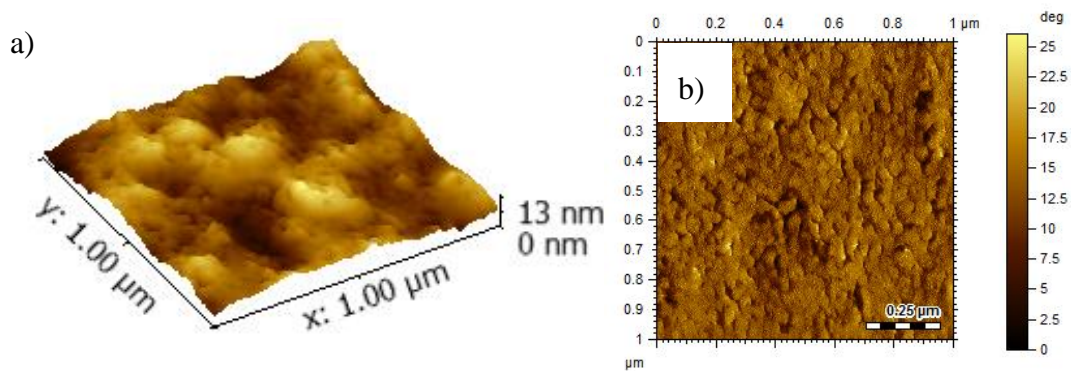


Figure 3-10. a) Topography and b) phase image for SIBS 68-5.

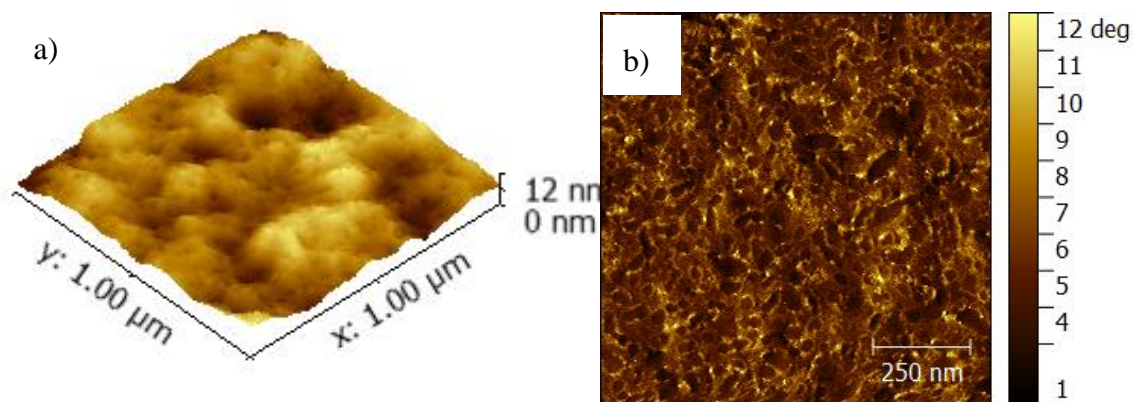


Figure 3-11. a) Topography and b) phase image for SIBS 68-7.

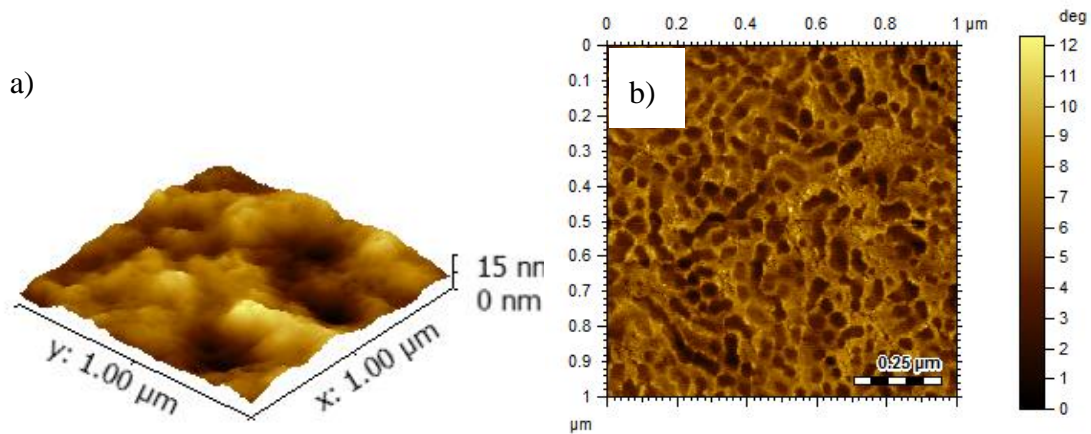


Figure 3-12. a) Topography and b) phase image for SIBS 68-9.

Therefore, AFM results clearly show that variations in the sulfonation level and polymer concentration have an effect on the morphology of the films, and more specifically, by showing a transition from circles and short cylinders to long and well-defined cylinders. A potential explanation for these results could be that it is an effect of the greater number of interconnections between the sulfonic groups as the ionic content increases in the films.

3.4 ELECTRICAL CHARACTERIZATION

As mentioned in the introduction, SIBS block copolymers have been previously studied for applications such as fuel cells, protective clothing, and biomedical devices. For this purpose, the mechanical, transport, and thermal properties, along with the biocompatibility of SIBS block copolymers, have been thoroughly investigated.²²⁻²⁶ Despite being the subject of several investigations, the electrical properties of SIBS had not been explored prior to the present study. In this section, the influence of the frequency of an applied electric field, and the effect of the degree of sulfonation and the polymer concentration on the dielectric constant and loss tangent of SIBS thin films are discussed.

3.4.1 EFFECT OF FREQUENCY

The dielectric constant and dielectric loss of SIBS thin films were characterized as a function of frequency in the range from 100 kHz to 1 MHz using a Network Analyzer. Figure 3-13 and Figure 3-14 show the dependence of the dielectric constant and loss tangent, respectively, on the frequency of an applied electric field for SIBS 91-7%. The results show that as the frequency increases the dielectric constant decreases. More specifically, the dielectric constant decreases from 7100 at 100 kHz to 4750 at 1 MHz (an approximate reduction of 33% from the base case). Similarly, as seen in Figure 3-14, the loss tangent significantly decreases with the frequency of the applied electric field from 1.9 at 100 kHz to 0.4 at 1 MHz.

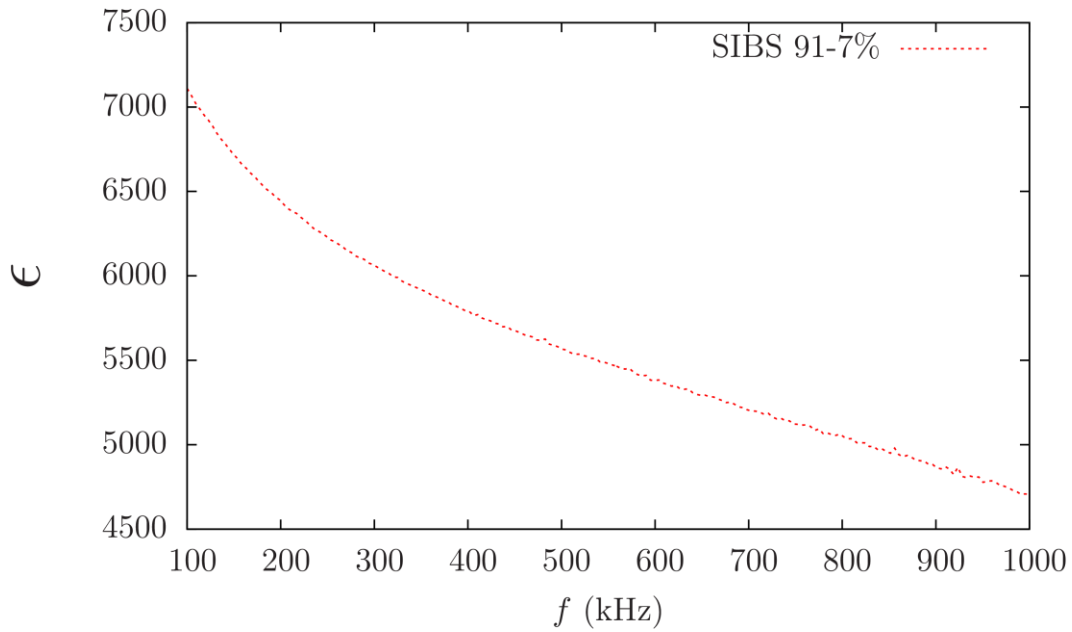


Figure 3-13. Dielectric constant of SIBS 91-7% as a function of frequency.

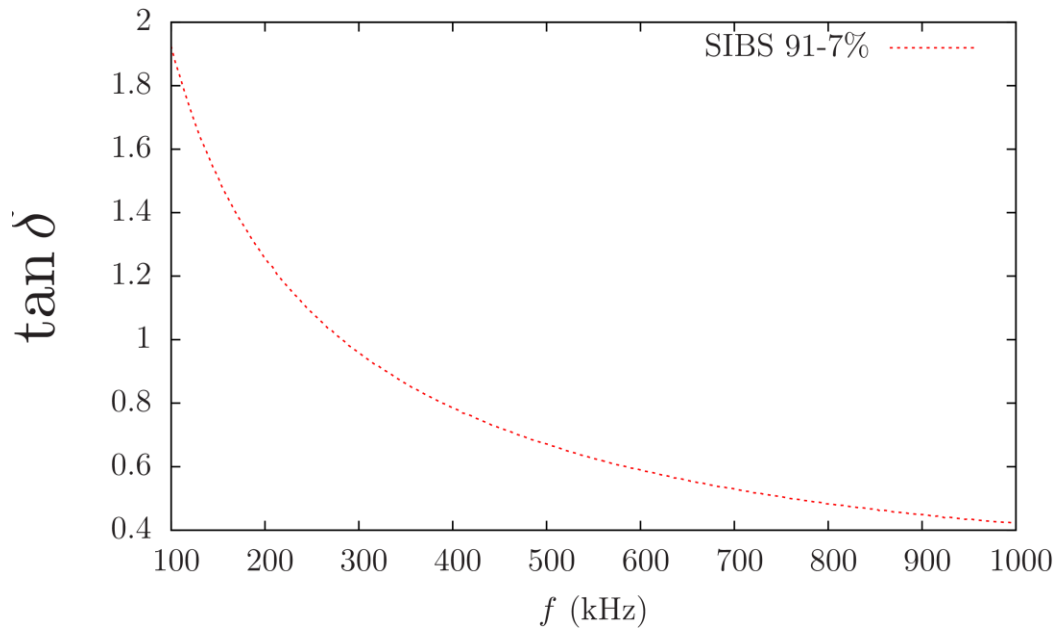


Figure 3-14. Loss tangent of SIBS 91-7% as a function of frequency.

Overall, these findings are in agreement with the theory of dielectric polarization, which identifies three potential mechanisms: electronic, distortion, and orientation polarization. Each mechanism corresponds to different phases of polarization that are present in a material

at specific frequencies. Figure 3-15 depicts a schematic of the governing mechanisms typically associated with each frequency range of an applied electric field. Moreover, the trend indicates that as the frequency increases, some of the mechanisms no longer have an effect in the dielectric constant and its value, therefore, decreases. Since the frequencies in this study are in the range of 100 kHz to 1 MHz, the most likely mechanism that dominates the process is the orientation polarization. The orientation polarization is caused by the rotation of dipoles or by the displacement of ions as they orient themselves with respect to the direction of the applied electric field.²⁷ Along that line of thought, it is important to note that the PS and PIB monomers in the SIBS polymer have very low and/or null dipole moments. Therefore, these are not expected to have an influence over the electrical properties as a function of frequency. However, the sulfonated SIBS polymers used in this study have sulfonic groups of ionic nature, which are likely responsible for the high dielectric constant values measured for these systems and the orientation polarization effects observed in the corresponding frequency range.

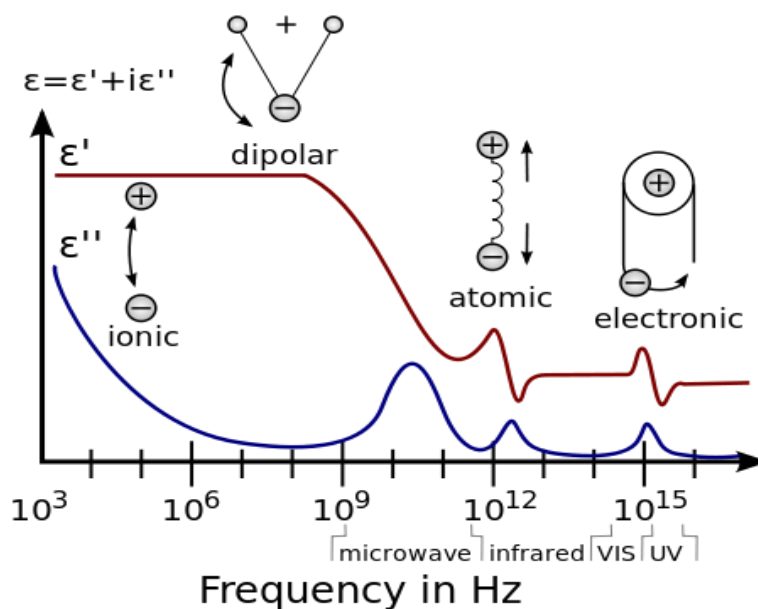


Figure 3-15. Typical polarization mechanisms observed over a range of frequencies.²⁷

Source: Kohl, P. a. Low-Dielectric Constant Insulators for Future Integrated Circuits and Packages. *Annu. Rev. Chem. Biomol. Eng.* **2011**, 2, 379–401 DOI: 10.1146/annurev-chembioeng-061010-114137.

The sulfonic groups tend to increase the polarization effect by their displacement under the influence of an electric field. Nevertheless, the displacement of these ions is limited in the SIBS films by steric effects such that these ions cannot displace synchronously with the oscillating electric field, and thus cause a reduction in the electrical properties as the frequency increases. J. Qian and collaborators found analogous findings with elastomers of polyacrylate, where a significant reduction in the dielectric constant is observed with frequency.²⁸

3.4.2 EFFECT OF SULFONATION

Sulfonated block copolymers such as polyether ether ketone, poly(phenylene-oxide), and polysulfones, among others, are different types of ionomeric materials that have been investigated for their use as fuel cell membranes. By modifying the amount of sulfonic groups (ionic content), the morphology, thermal, mechanical, and transport properties can be controlled to achieve a desired performance. Particularly for SIBS, the inclusion of the sulfonic groups into the PS phase, corresponding to approximately 30% by weight in this study, leads to changes in the morphology, its chemical nature, and could result in a variety of different applications for the polymer. The objective of this section, therefore, is to determine how the changes in ionic content affect the electrical properties of the sulfonated SIBS thin films.

Figure 3-16 and Figure 3-17 show the dielectric constant and loss tangent, respectively, for SIBS films with polymer concentration of 7 wt% and different sulfonation levels, namely, 55%, 68%, and 91%.

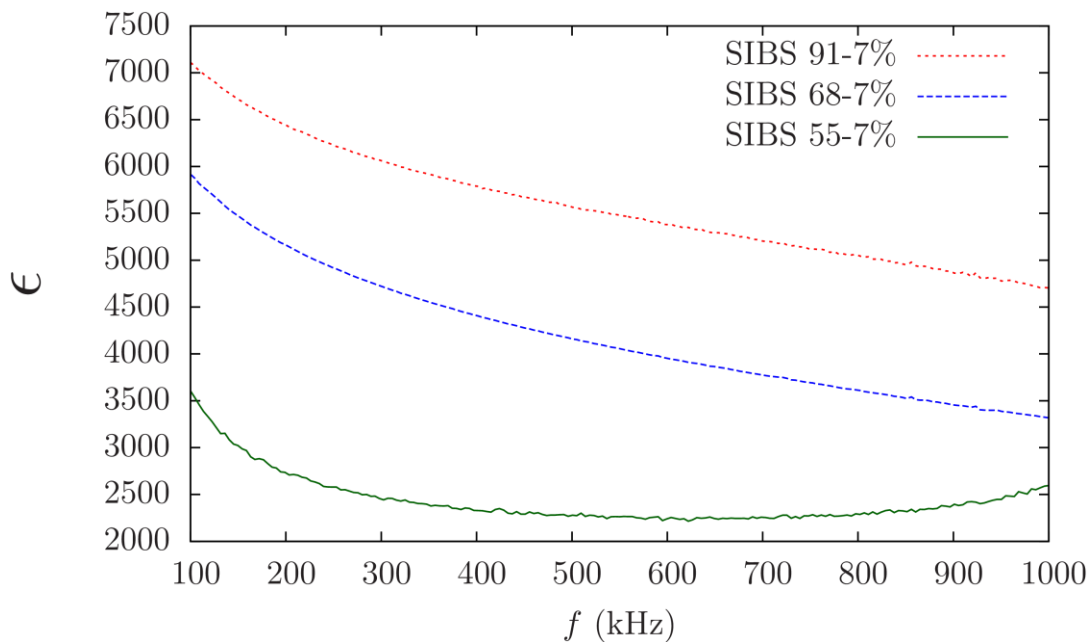


Figure 3-16. Dielectric constant for SIBS thin films as a function of the sulfonation level.

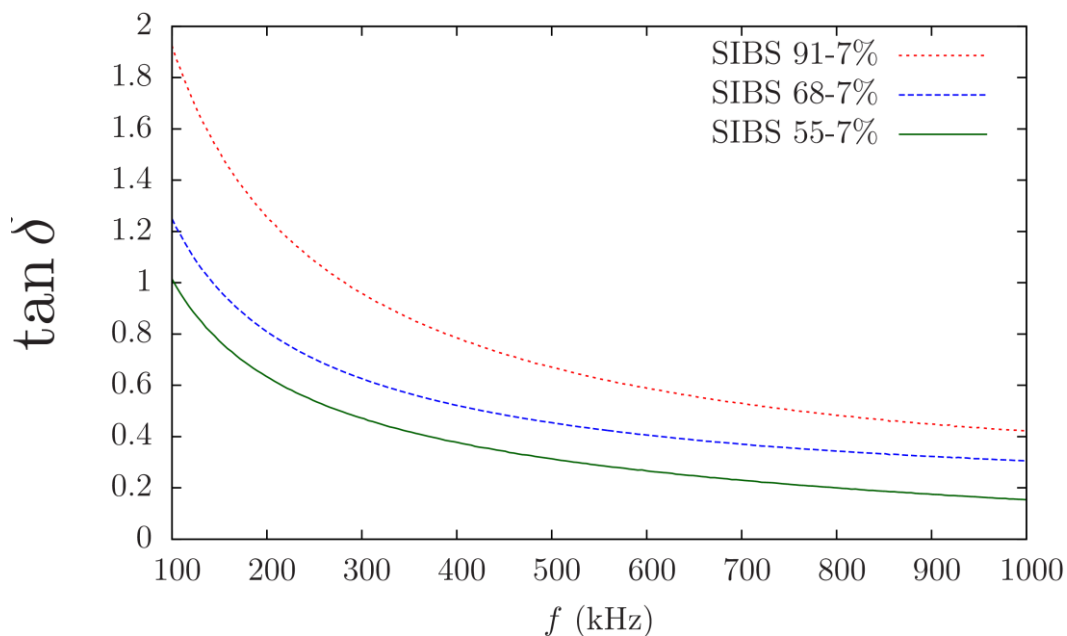


Figure 3-17. Loss tangent for SIBS thin films as a function of the sulfonation level.

The results show that both, the dielectric constant and loss tangent, increase with the sulfonation level in the SIBS thin films. More specifically, from Figure 3-16, the dielectric constant values at 100 kHz for SIBS 55-7, SIBS 68-7, and SIBS 91-7, were measured at 3602, 5916, and 7110, respectively. A possible explanation for these observations could be the formation of multiplets and the affinity of sulfonic groups to water.

Multiplets are aggregates of ion pairs, which were first introduced by Einsenberg,²⁹ and their formation depends on the electrostatic forces between ions and the characteristics of the polymer matrix. It is well known that the interaction strength among multiplets is greater for small and polar ion pairs.^{30,31} As the ionic content increases within the polymer (e.g. via sulfonation), the formation of larger aggregates is promoted owing to the greater electrostatic interactions between the ions. The polymer that surrounds the multiplets becomes attached to them thus leading to a loss of the mobility of the polymer backbone. The polymers that surround the multiplets comprise a continuous phase (or cluster); whereas, the multiplets constitute a segregated phase, also known as ionic domains.^{32,29}

The presence of ionic domains, derived from the sulfonation treatment, explains why the SIBS thin films exhibit large dielectric constants on account of the polarization of these domains by an external electric field. These observations are also in agreement with the AFM results that show that the ionic domains grow in size as the sulfonation level increases. These findings are also consistent with those of Butckewitsch & Scheinbeim,⁵ who studied the dielectric properties of sulfonated poly(styrene-ethylene-styrene) (SEBS) membranes, and found an enhancement of the dielectric constant with increasing sulfonation levels. Another contributing factor to the high values of the dielectric constant is that the water absorbed by the sulfonated SIBS films and its constituent solvents have large dielectric constants, which are expected to contribute to the overall dielectric properties of the SIBS films.

The loss tangent is observed to decrease with increasing frequencies of the applied electric field, regardless of the sulfonation level (Figure 3-17). Moreover, the degree of sulfonation has a tendency to shift upward the curve of the loss tangent. Particularly, at a fixed frequency of 100 kHz the loss tangent values for SIBS 55-7, SIBS 68-7, and SIBS 91-7 are 1.015, 1.250 and 1.925, respectively. This tendency is opposite to the expected behavior because of the inverse proportionality of the loss tangent with the dielectric constant, as shown by equation 7:

$$\tan \delta = \frac{1}{\rho_{SIBS} \omega \epsilon_r \epsilon_0} \quad (\text{Equation 7})$$

At higher sulfonation percentages, the dielectric constant increases. Therefore, if the resistivity of the film remained invariant with the sulfonation level, the loss tangent should decrease (as indicated by Equation 7). Contrary to the aforementioned expectations, the loss tangent increases with the sulfonation level (Fig. 3-17), thus indicating that the resistivity of the film is likely decreasing with increasing sulfonation.

Figure 3-18 shows the resistivity of the SIBS thin films at the different sulfonation levels. It exhibits an inverse proportionality with the sulfonation level; hence, as the sulfonation increases, there is less opposition to the current flow offered by the film. These results can

be correlated with the phase images (Figure 3-7 to Figure 3-9) that show an increment in the continuous regions for SIBS 91 as compared to the SIBS 55 and SIBS 68 films.

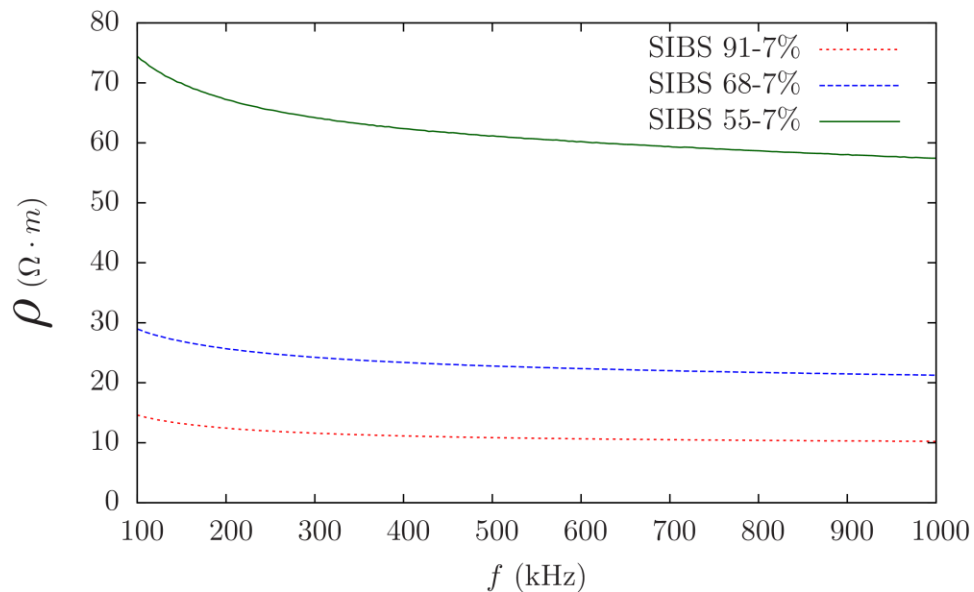


Figure 3-18. Resistivity for SIBS thin films as a function of the sulfonation level.

Noting these results, the dielectric losses for the SIBS films are quite high at the lowest frequency studied (100 kHz). Therefore, it is expected that the material will dissipate much heat in this regime. This, in turn, could have a negative impact on the applicability of SIBS films into electronic devices that operate at low frequencies.

3.4.3 EFFECT OF POLYMER CONCENTRATION

The results for the dielectric constant and loss tangent of SIBS 68 as function of polymer concentration are shown in Figure 3-19 and Figure 3-20, respectively. It can be observed that as the polymer concentration increases from 5 wt% to 9 wt%, the dielectric constant increases as well. This suggests a direct proportionality of the dielectric constant with the polymer concentration in this range. Values for the dielectric constant at 100 kHz are 2000, 5900, and 7500 for SIBS 68-5%, SIBS 68-7%, and SIBS 68-9%, respectively.

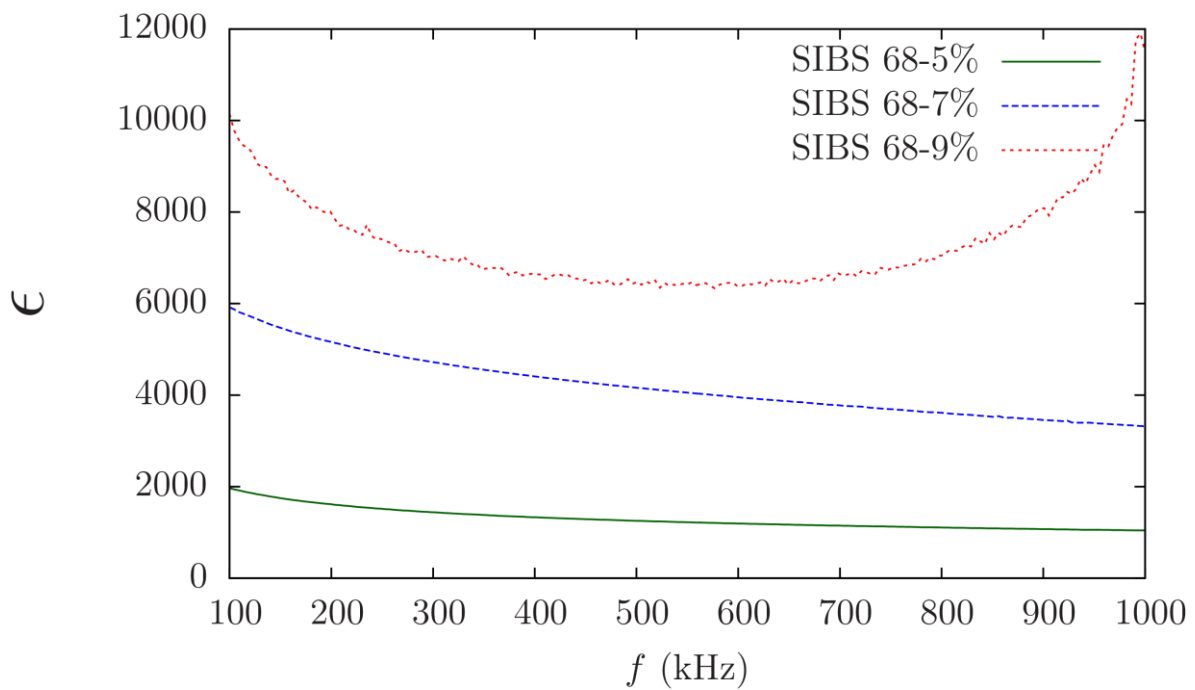


Figure 3-19. Dielectric constant vs. frequency as a function of polymer concentration for SIBS 68.

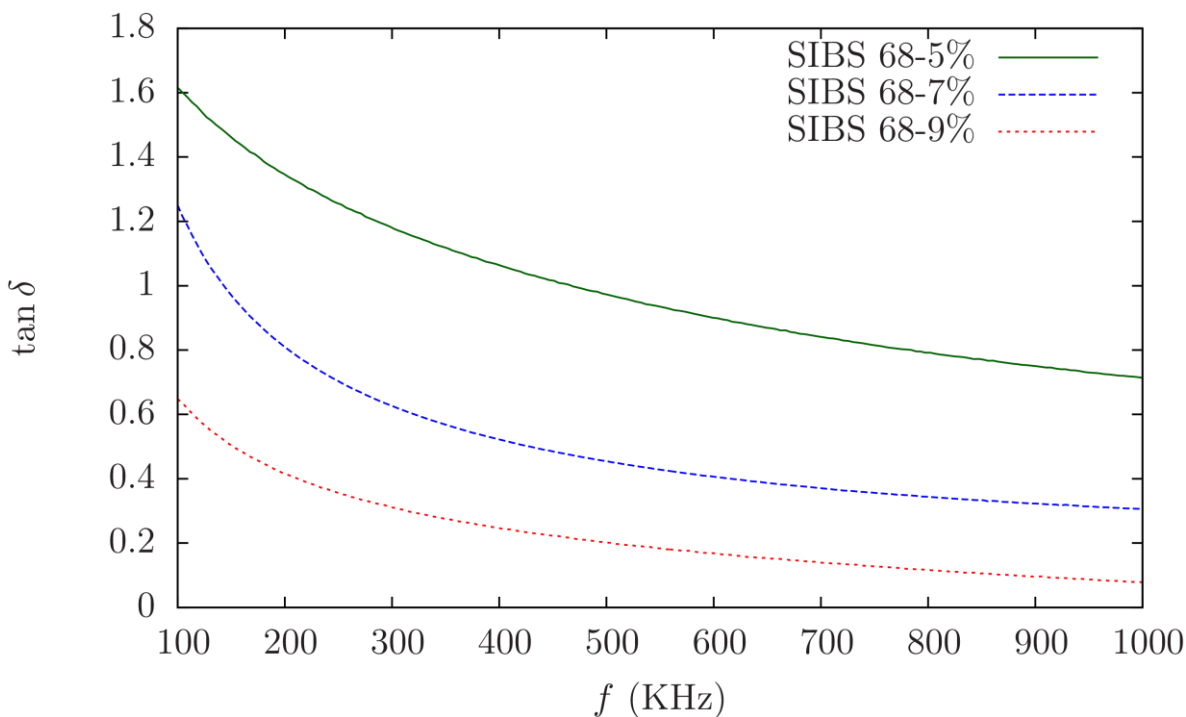


Figure 3-20. Loss tangent vs. frequency as a function of polymer concentration for SIBS 68.

A possible explanation for these results could be that for low polymers concentrations there is more distance between ion pairs, which thus hinders the formation of multiplets. As the polymer concentration increases, there are more ion pairs that are closer and experience stronger electrostatic interactions. The previously presented phase images for SIBS 68-5%, SIBS 68-7%, and SIBS 68-9% showed changes in morphology from short cylinders and circles to more defined and longer cylinders, which could support the formation of the multiplets or ionic domains responsible for the increase in the dielectric constant.

A particular observation from Figure 3-19, is that for SIBS 68-9%, as the frequency increases, the dielectric constant increases as well, which is not the expected behavior. A possible explanation for this could be that the different morphology of SIBS 68-9% could affect to some extent the contact between the polymer and the electrodes of the MIM capacitor. It could be that, once the electric field is applied, charged particles get accumulated in this interfacial region and additional polarization, not necessarily corresponding to the polymer, is observed.²⁸ This effect is also observed for samples of SIBS 91-9% as shown in Figure

3-21, which could be an indication that at this polymer concentration the properties of SIBS change substantially and thus promote the observed effect.

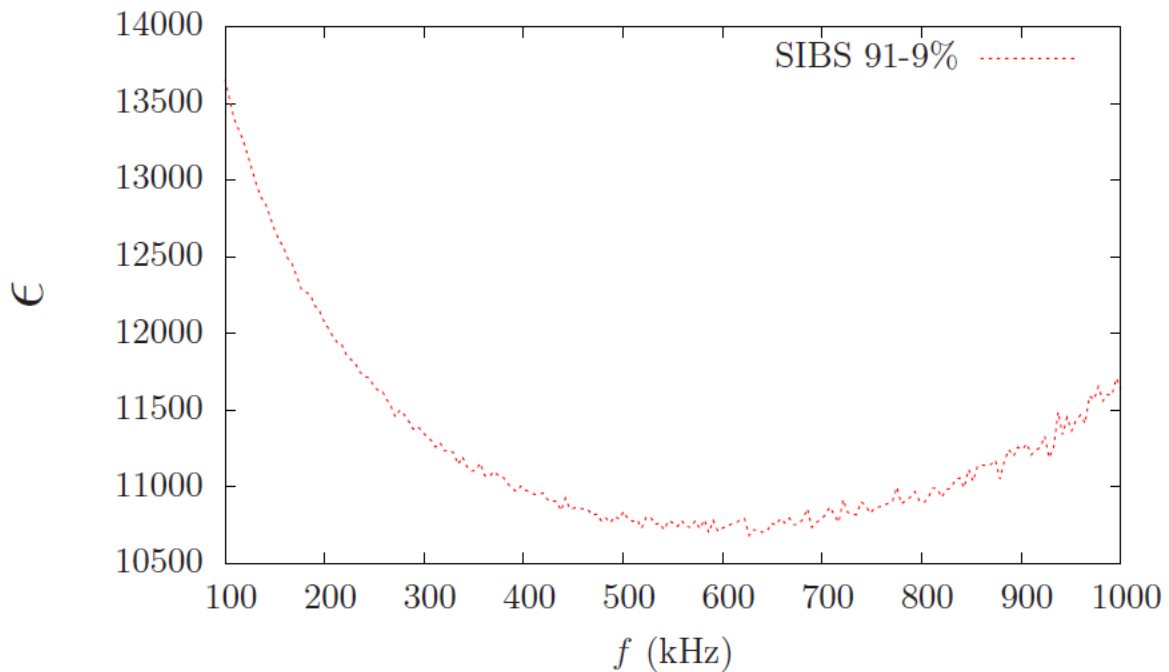


Figure 3-21. Dielectric constant vs. frequency for SIBS 91-9%.

Finally, an inverse proportionality is observed between the loss tangent and the polymer concentration, that is, the loss tangent decreases with increasing polymer concentration. According to equation 7, this therefore suggests that the dielectric constant has a more relevant effect on loss tangent as compared to the resistivity when the polymer concentration is varied. And as such, Figure 3-22 confirms that the resistivity does not exhibit significant changes with the polymer concentration.

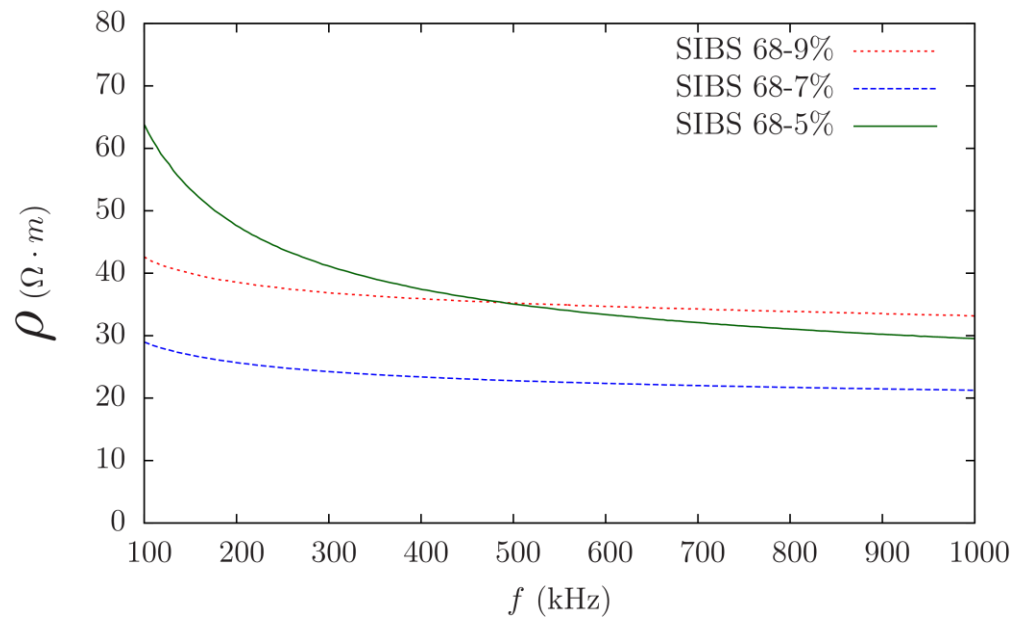


Figure 3-22. Resistivity as a function of polymer concentration for SIBS 68.

3.4.4 VARIABILITY IN THE ELECTRICAL PROPERTIES

Each fabricated sample of SIBS thin film consists of approximately 100 MIM capacitors evenly distributed across the surface of the substrate. We have taken this advantageous setup to generate contour plots to provide a qualitative description of the distribution of the electrical properties in the SIBS films.

In order to improve the visuals of the contour plots, the electrical properties are normalized with respect to the average from the ensemble of capacitors, such that the variations in the normalized properties fall in a scale that ranges from 0 to 3 (the latter being the maximum value). As one may expect, the average depends on the polymer concentration and sulfonation level; therefore, the average property is conveniently reported in the surface plots to provide some qualitative sense of the extent of these variations.

Figure 3-23 to Figure 3-28 show the dielectric constant and loss tangent as a function of the polymer concentration for SIBS 91 and at a frequency of 550 kHz, which corresponds to a middle point in the frequency range considered in this study.

SIBS 91-5% and SIBS 91-9% exhibit a nearly uniform distribution of the dielectric constant across the film. In comparison, SIBS 91-7% shows a region of pronounced peaks that indicates greater values of dielectric constant. Interestingly, for the polymer concentrations evaluated, the films presented only slight variations in the loss tangent.

In general, some degree of variability can be seen at the surface maps, which may indicate that there are some regions of relatively lower or higher ionic content than the average, as well as small variations in the thickness of the films.

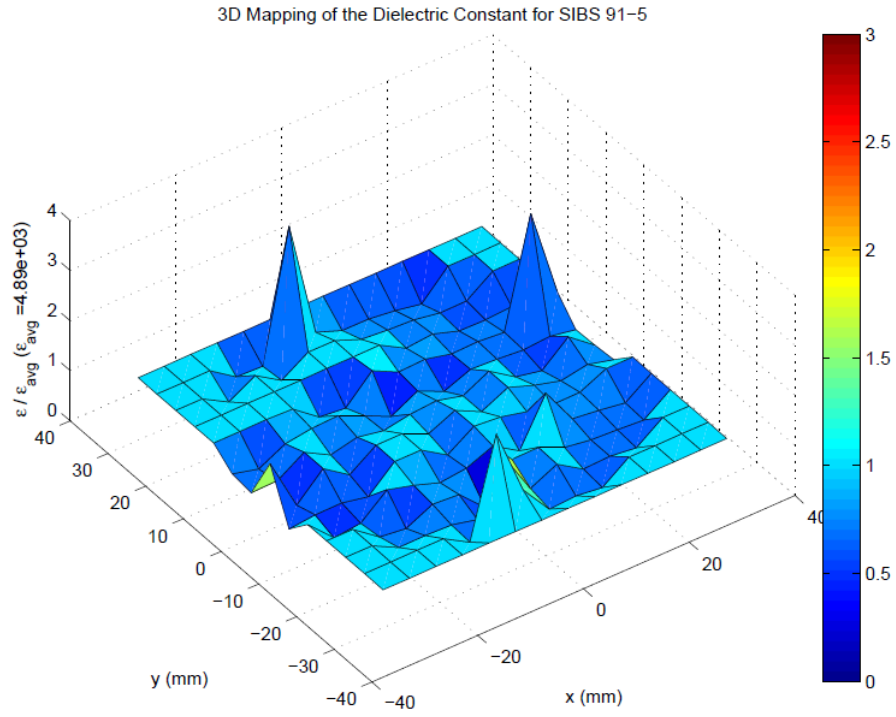


Figure 3-23. Surface plot of dielectric constant for SIBS 91-5% at 550 kHz.

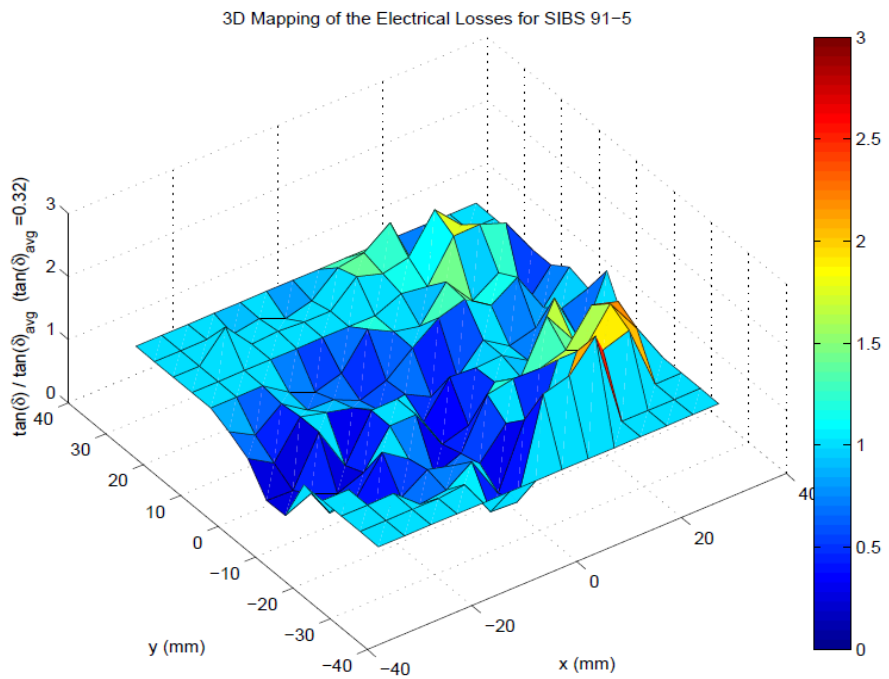
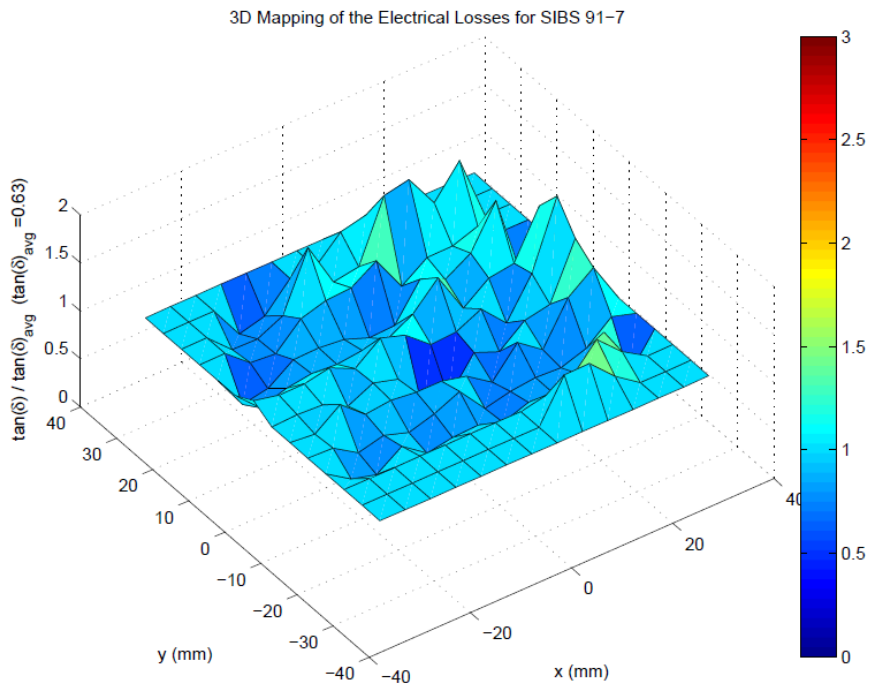
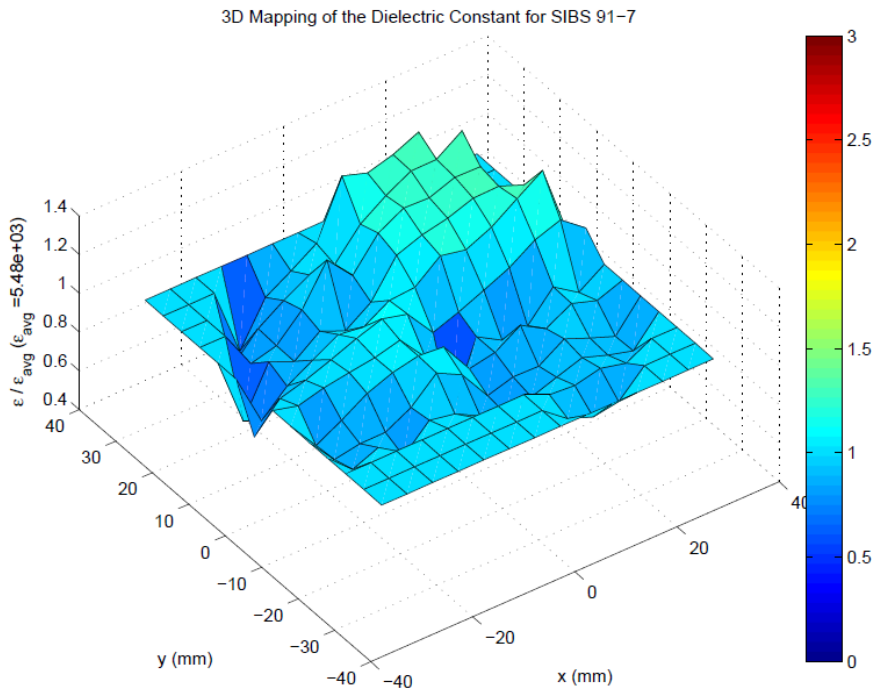


Figure 3-24. Surface plot of the loss tangent for SIBS 91-5% at 550 kHz.



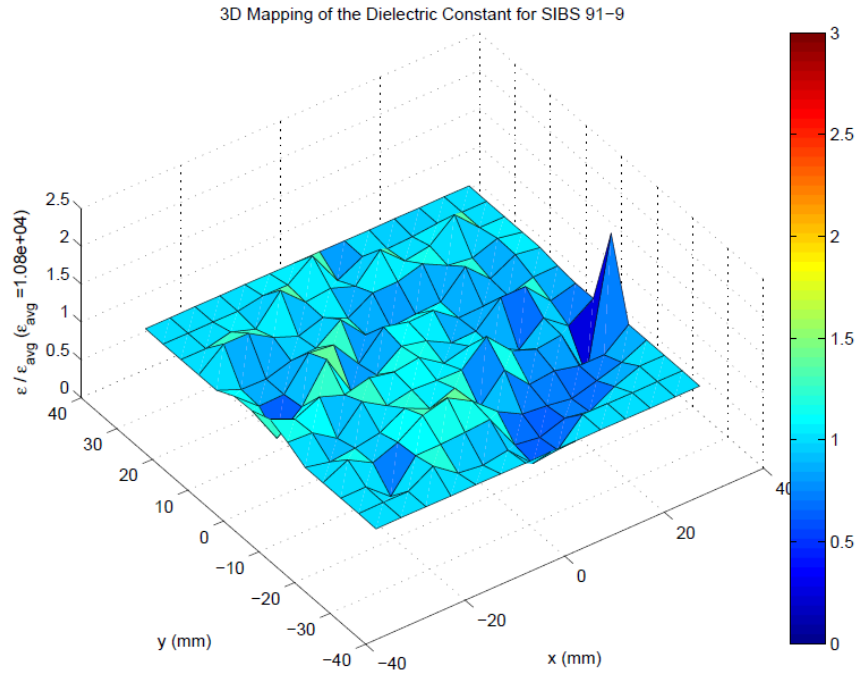


Figure 3-27. Surface plot of the dielectric constant for SIBS 91-9% at 550 kHz.

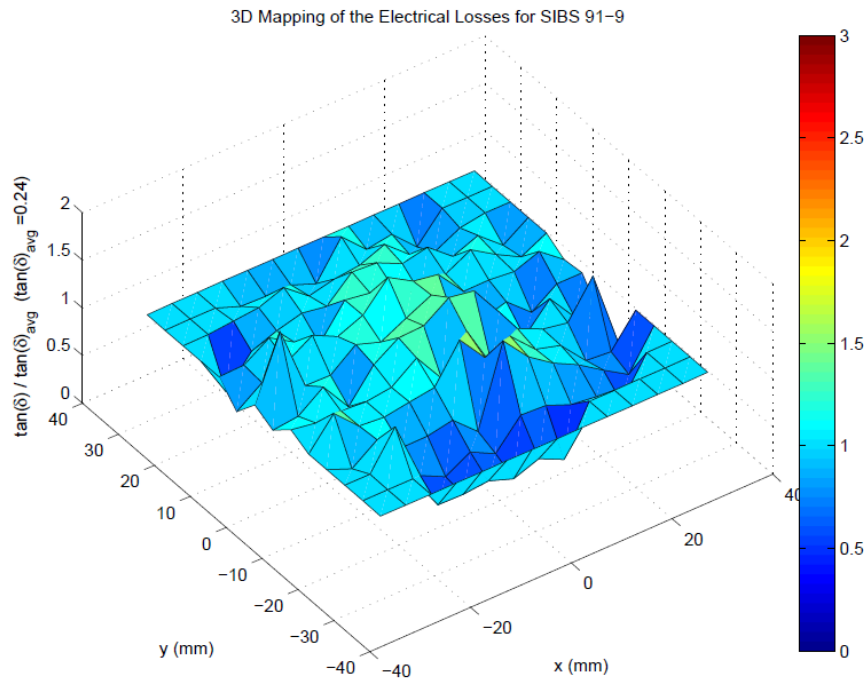


Figure 3-28. Surface plot of the loss tangent for SIBS 91-9% at 550 kHz.

3.4.5 REPRODUCIBILITY OF THE ELECTRICAL PROPERTIES

Two replicates of SIBS 91 were performed at concentrations of 5 wt% and 7 wt% in order to characterize the electrical properties of the films. The results of the electrical characterization are presented in boxplots to elucidate the most representative statistical points and to evaluate the dispersion of the data. The boxplots were generated at three different frequencies, however, only the results for two frequencies are shown because the same tendency is observed for the third frequency.

The dispersion of the data for replicates of SIBS 91-5% at 100 KHz and 401.5 KHz are shown in Figure 3-29 and Figure 3-30, respectively. From Figure 3-29, it can be inferred that for both replicates the data is not dispersed. However, there are some outliers that do not represent the tendency of the majority of the data. The means of the replicates are about 5000 and 7500 for SIBS 91-5 and SIBS 91-5R1, respectively.

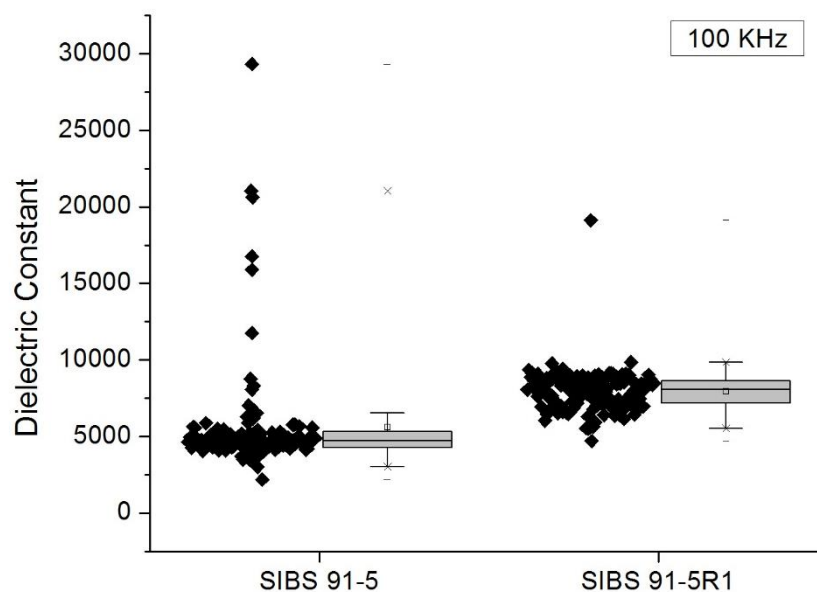


Figure 3-29. Dielectric constant of replicates of SIBS 91-5% at 100 KHz

In Figure 3-30, the data at 401.5 kHz is more dispersed than at 100 kHz. The means decrease to 3500 and 6000 for SIBS 91-5 and SIBS 91-5, respectively, as an effect of the increment in frequency.

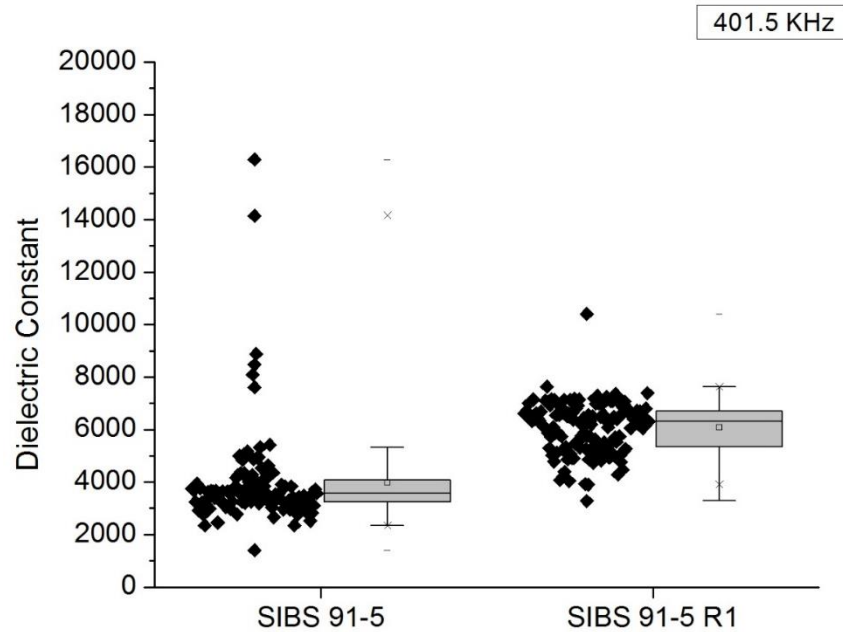


Figure 3-30. Dielectric constant for replicates of SIBS 91-5% at 401.5 kHz.

The data for replicates SIBS 91-7 and SIBS 91-7R1 at 100 kHz and 401.5 kHz is presented in Figure 3-31 and Figure 3-32. The data is quite dispersed for both replicates, regardless the frequency, but it is contained within the boxplots, which means that no outliers are observed.

The means for SIBS 91-7 and SIBS 91-7 R1 at 100 kHz are about 7000 and 9000, respectively. As expected at 401.5 kHz, the means were reduced to 5500 and 7000 approximately, for SIBS 91-7 and SIBS 91-7 R1, respectively.

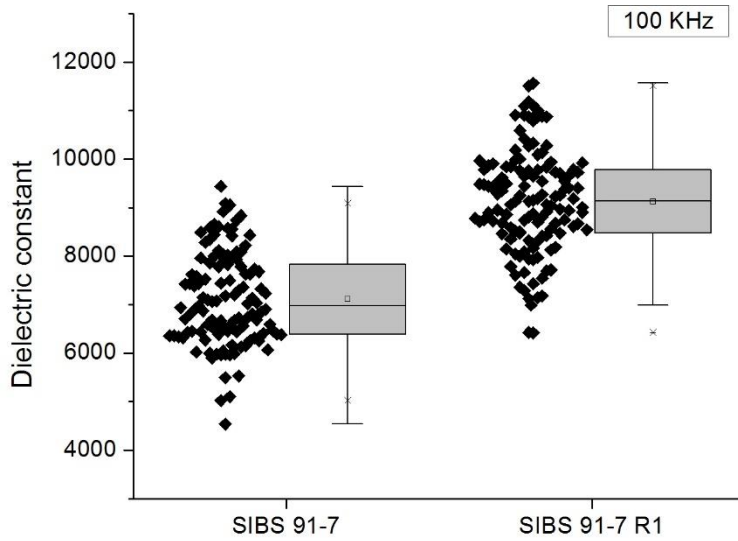


Figure 3-31. Dielectric constant for replicates of SIBS 91-7% at 100 kHz.

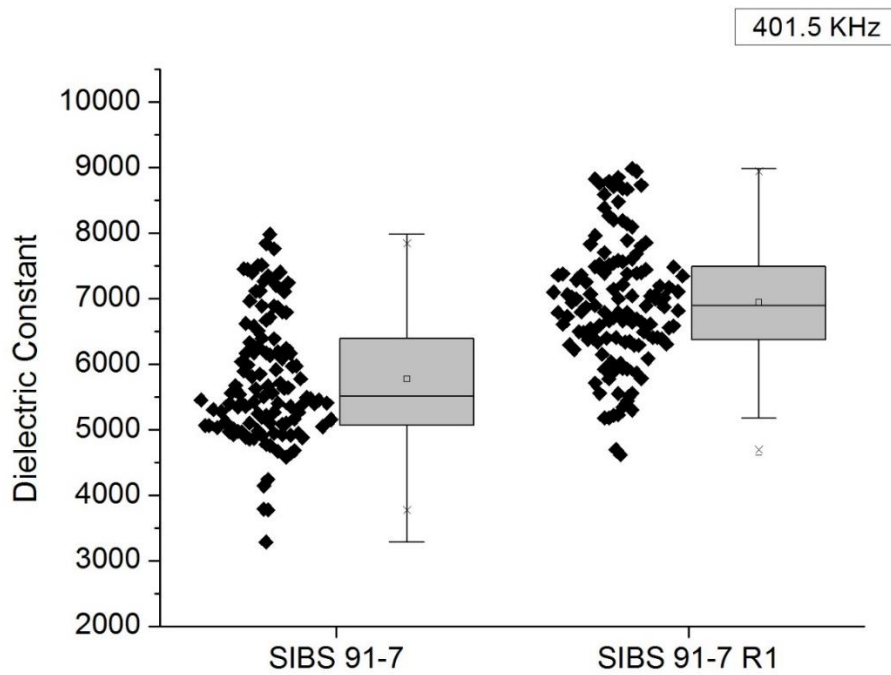


Figure 3-32. Dielectric constant for replicates of SIBS 91-7% at 401.5 kHz.

The figures show that the variance between the pair of replicates is substantial. In order to confirm this, we performed 2t sample statistical tests on the data. The statistical test revealed

no correlation between the replicates, since the p-values were zero; thus indicating that there is a significant statistical difference between the pair of samples tested. That is, the values of the electrical properties differed significantly (from a statistical point of view).

Table 5. Results of 2t sample test for replicates of SIBS 91-5% and SIBS 91-7%.

REPLICATES	P-value	Null hypothesis	Alternative hypothesis
SIBS 91-5/SIBS 91-5R1 100 kHz	0.000	Rejected	Accepted
SIBS 91-5/SIBS 91-5R1 401.5 kHz	0.000	Rejected	Accepted
SIBS 91-7/SIBS 91-7R1 100 kHz	0.000	Rejected	Accepted
SIBS 91-7/SIBS 91-7R1 401.5 kHz	0.000	Rejected	Accepted

A possible explanation for the observed differences in electrical properties between the pair of replicates is that the film thickness for the replicates is about twice the thickness as compared to the original samples. It could be, therefore, inferred that the polymer used for the replicates had absorbed a significant amount of water (on account of the greater film thickness) as a result of the fact that it had been exposed to ambient conditions for a longer period of time in comparison with the original samples. These observations could potentially explain the higher values of the electrical properties measured for the films. In a future investigation, additional studies should be performed to determine the effect of time on the materials properties in order to ensure appropriate performance.

4 CONCLUSIONS

This investigation principally aimed to characterize the electrical properties (dielectric constant and loss tangent) of sulfonated poly(styrene-isobutylene-styrene) SIBS thin films as a function of the polymer concentration and the sulfonation level. The polymer concentrations considered in this study are: 5 wt%, 7 wt%, and 9 wt%; and the sulfonation levels are: 55%, 68%, and 91%. To perform the electrical characterization, metal-insulator-metal (MIM) capacitors were fabricated and an ac electric field with frequency range from 100 kHz to 1 MHz was applied.

The results showed that the dielectric constant of the SIBS thin films increases with the sulfonation level. The curves for the dielectric constant shifted upward as the sulfonation percentage increased within the films. Under the sulfonation levels considered in this study, the dielectric constant of the SIBS thin films did not reach a maximum value (or saturated). It is suspected that the dielectric constant should saturate or possibly decrease at even higher sulfonation levels. The enhancement of the dielectric constant with the level of sulfonation is attributed to the fact that sulfonic groups are ionic agents that exhibit a certain degree of polarization under the application of an electric field. It is inferred that the underlying mechanism attributed to the decay in dielectric constant with increasing frequencies is orientation polarization, which is a plausible explanation given that this mechanism is known to be influential in the range of frequencies considered in this study.

Another contributing factor to the high values of the dielectric constant observed for the SIBS thin films is the incorporation of substances of high dielectric constant within the material. Bearing in mind that the preparation of SIBS thin films requires dissolution of SIBS with some polar solvents, such as hexyl alcohol, its presence is suspected to also account for the high dielectric constant measured for the films. It is important to mention that the amount of polar solvents within the SIBS films was unknown during the experiments, and therefore, it is difficult to quantify its specific impact on the dielectric constant. Additionally, sulfonic groups have a strong affinity to water, which is yet another substance with a high dielectric

constant that may have been present during the electrical characterization studies. It is key to note that the presence of solvents and water was confirmed by the TGA measurements. Despite knowing the total weight loss from the solvents and water from the TGA experiments, their composition cannot be determined by this technique. Without a separate chemical analysis, it is difficult to quantify the contribution of the solvents and water to the total dielectric response of the SIBS thin films. It is also possible that the interaction of the water and solvent molecules with the sulfonic groups contribute somehow to the dielectric properties of the sulfonated SIBS thin films. If that is the case, it may prove challenging to provide an estimate of the effect of the solvent and water on the dielectric properties. An estimate only based on the amount of solvent and water present may underestimate the total effect.

The dielectric constant of the SIBS thin films increased with the polymer concentration at a constant sulfonation level. The AFM images revealed that an increasing polymer concentration brings morphological changes that favor the enhancement of the dielectric properties of the SIBS films. For instance, the ionic domains (accountable for the augmentation in dielectric properties) increase in size with the concentration of the polymer. Particularly, at the maximum polymer concentration considered in this study (9 wt%), some extent of interconnection between the ionic channels is observed from the AFM results. One may infer that the mean distance between pair of ions (or multiplets) decreases with greater polymer concentrations leading to an increment in the polarization effect on account of the greater electrostatic forces.

The loss tangent curves for SIBS thin films tend to shift upward with increasing levels of sulfonation. This was attributed to the effect of sulfonation on the resistivity of the SIBS thin films: as the sulfonation increased, the resistivity decreased leading to higher values of loss tangent. On the contrary, when the polymer concentration was varied from 5 wt% to 9 wt%, changes in resistivity were not significant and thus, the main contribution to the loss tangent was determined by the dielectric constant, which ultimately led to lower loss tangent for higher polymer concentration.

It was also observed that loss tangent decreased with the frequency of the applied electric field at the sulfonation levels considered in this study. This makes the sulfonated SIBS thin films suitable for applications at high frequencies owing to the reduced heat dissipation effects (smaller loss tangent).

Finally, it is important to note that the TGA results showed that the thermal stability of SIBS increases with the level of sulfonation. This is a factor of potential interest when evaluating the applicability of SIBS films for engineering applications, such as, the design of novel electrical devices, biomedical applications, and protective clothing.

5 REFERENCES

- (1) Borbely, A.; Kreider, J. F.; Bejan, A.; Cundiff, J. S.; Davis, L. R. *The MEMS Handbook: MEMS: Design and Fabrication*; Gad-el-Hak, M., Ed.; Second.; CRC Taylor & Francis: Boca Raton, FL, 2006.
- (2) Webster, J. R.; Elshabini, A. *Thin Film Polymer Dielectrics for High-Voltage Applications under Severe Environments* Thin Film Polymer Dielectrics for High-Voltage Applications under Severe Environments, Virginia Polytechnic Institute and State University, 1998.
- (3) Maier, G.; Garching, D.-. Low dielectric constant polymers for microelectronics. *Prog. Polym. Sci.* **2001**, *26*, 3–61.
- (4) Dang, Z.-M.; Yuan, J.-K.; Zha, J.-W.; Zhou, T.; Li, S.-T.; Hu, G.-H. Fundamentals, processes and applications of high-permittivity polymer–matrix composites. *Progress in Materials Science*, 2012, *57*, 660–723.
- (5) Butkewitsch, S.; Scheinbeim, J. Dielectric properties of a hydrated sulfonated poly(styrene–ethylene/butylenes–styrene) triblock copolymer. *Appl. Surf. Sci.* **2006**, *252*, 8277–8286 DOI: 10.1016/j.apsusc.2005.10.059.
- (6) Connor, K. A. O.; Smith, J.; Curry, R. D. DIELECTRIC CHARACTERIZATION OF POLYMER-CERAMIC. *IEEE Instrum. Meas. Mag.* **2009**, 336–341.
- (7) Schumacher, B.; Geßwein, H.; Haußelt, J.; Hanemann, T. Temperature treatment of nano-scaled barium titanate filler to improve the dielectric properties of high-k polymer based composites. *Microelectron. Eng.* **2010**, *87*, 1978–1983 DOI: 10.1016/j.mee.2009.12.018.
- (8) Liu, A.; Wang, X.; Wang, L.; Wang, H.; Wang, H. POLYMER Prediction of dielectric constants and glass transition temperatures of polymers by quantitative structure

- property relationships. *Eur. Polym. J.* **2007**, *43*, 989–995 DOI: 10.1016/j.eurpolymj.2006.12.029.
- (9) Basu, D.; Das, A.; Stöckelhuber, K. W.; Jehnichen, D.; Formanek, P.; Sarlin, E.; Vuorinen, J.; Heinrich, G. Evidence for an in Situ Developed Polymer Phase in Ionic Elastomers. *Macromolecules* **2014**, *47*, 3436–3450 DOI: 10.1021/ma500240v.
- (10) Li, N.; Guiver, M. D. Ion transport by nanochannels in ion-containing aromatic copolymers. *Macromolecules* **2014**, *47*, 2175–2198 DOI: 10.1021/ma402254h.
- (11) Liu, Y.; Ghaffari, M.; Zhao, R.; Lin, J. H.; Lin, M.; Zhang, Q. M. Enhanced electromechanical response of ionic polymer actuators by improving mechanical coupling between ions and polymer matrix. *Macromolecules* **2012**, *45*, 5128–5133 DOI: 10.1021/ma300591a.
- (12) Suleiman, D.; Napadensky, E.; Sloan, J. M.; Crawford, D. M. Thermogravimetric characterization of highly sulfonated poly(styrene–isobutylene–styrene) block copolymers: Effects of sulfonation and counter-ion substitution. *Thermochim. Acta* **2007**, *460*, 35–40 DOI: 10.1016/j.tca.2007.05.012.
- (13) Avilés-Barreto, S. L.; Suleiman, D. Transport properties of sulfonated poly (styrene–isobutylene–styrene) membranes with counter-ion substitution. *J. Appl. Polym. Sci.* **2013**, *129*, 2294–2304 DOI: 10.1002/app.38952.
- (14) Vazquez-Mena, O.; Sidler, K.; Savu, V.; Park, C. W.; Guillermo Villanueva, L.; Brugger, J. Reliable and improved nanoscale stencil lithography by membrane stabilization, blurring, and clogging corrections. *IEEE Trans. Nanotechnol.* **2011**, *10*, 352–357 DOI: 10.1109/TNANO.2010.2042724.
- (15) Vazquez-Mena, O.; Gross, L.; Xie, S.; Villanueva, L. G.; Brugger, J. Resistless nanofabrication by stencil lithography: A review. *Microelectron. Eng.* **2015**, *132*, 236–254 DOI: 10.1016/j.mee.2014.08.003.

- (16) Vazquez-Mena, O.; Sannomiya, T.; Tosun, M.; Villanueva, L. G.; Savu, V.; Voros, J.; Brugger, J. High-resolution resistless nanopatterning on polymer and flexible substrates for plasmonic biosensing using stencil masks. *ACS Nano* **2012**, *6*, 5474–5481 DOI: 10.1021/nn301358n.
- (17) Takano, N.; Doeswijk, L. M.; Van Den Boogaart, M. a F.; Brugger, J. Application of microstencil lithography on polymer surfaces for microfluidic systems with integrated microelectrodes. *Proc. 2006 Int. Conf. Microtechnologies Med. Biol.* **2006**, 139–142 DOI: 10.1109/MMB.2006.251511.
- (18) Nicolet, T.; All, C. *Introduction to Fourier Transform Infrared Spectrometry*; 2001.
- (19) Movil, O. A. THIN FILM PROCESSING AND THE MORPHOLOGICAL AND MECHANICAL CHARACTERIZATION OF SULFONATED POLY (STYRENE-ISOBUTYLENE-STYRENE) (SIBS), University of Puerto Rico, 2013.
- (20) Avilés-Barreto, S. L. FUNCTIONALIZATION AND CHARACTERIZATION OF SULFONATED POLY(STYRENE-ISOBUTYLENE-STYRENE) MEMBRANES FOR FUEL CELLS AND SPECIALTY SEPARATION APPLICATIONS, University of Puerto Rico, 2014.
- (21) Smitha, B.; Sridhar, S.; Khan, a. a. Synthesis and characterization of proton conducting polymer membranes for fuel cells. *J. Memb. Sci.* **2003**, *225*, 63–76 DOI: 10.1016/S0376-7388(03)00343-0.
- (22) Storey, R. F.; Baugh, D. W. Poly(styrene-b-isobutylene-b-styrene) block copolymers produced by living cationic polymerization. Part III. Dynamic mechanical and tensile properties of block copolymers and ionomers therefrom. *Polymer (Guildf)*. **2001**, *42*, 2321–2330 DOI: 10.1016/S0032-3861(00)00658-3.
- (23) Antony, P.; Kwon, Y.; Puskas, J. E.; Kovar, M.; Norton, P. R. Atomic force microscopic studies of novel arborescent block and linear triblock polystyrene-

- polyisobutylene copolymers. *Eur. Polym. J.* **2004**, *40*, 149–157 DOI: 10.1016/j.eurpolymj.2003.08.010.
- (24) Hamley, I. W. Ordering in thin films of block copolymers: Fundamentals to potential applications. *Prog. Polym. Sci.* **2009**, *34*, 1161–1210 DOI: 10.1016/j.progpolymsci.2009.06.003.
- (25) Kopchick, J. G.; Storey, R. F.; Beyer, F. L.; Mauritz, K. a. Poly[acrylic acid-b-styrene-b-isobutylene-b-styrene-b-acrylic acid] pentablock terpolymers: 1. Morphological characterization. *Polymer (Guildf)*. **2007**, *48*, 3739–3748 DOI: 10.1016/j.polymer.2007.04.048.
- (26) Suleiman, D.; Padovani, A. M.; Negrón, A. a.; Sloan, J. M.; Napadensky, E.; Crawford, D. M. Mechanical and chemical properties of poly(styrene-isobutylene-styrene) block copolymers: Effect of sulfonation and counter ion substitution. *J. Appl. Polym. Sci.* **2014**, *131*, n/a – n/a DOI: 10.1002/app.40344.
- (27) Kohl, P. a. Low–Dielectric Constant Insulators for Future Integrated Circuits and Packages. *Annu. Rev. Chem. Biomol. Eng.* **2011**, *2*, 379–401 DOI: 10.1146/annurev-chembioeng-061010-114137.
- (28) Qiang, J.; Chen, H.; Li, B. Experimental study on the dielectric properties of polyacrylate dielectric elastomer. *Smart Mater. Struct.* **2012**, *21*, 025006 DOI: 10.1088/0964-1726/21/2/025006.
- (29) Eisenberg, a; Hird, B.; Moore, R. B. A new multiplet-cluster model for the morphology of random ionomers. *Macromolecules* **1990**, *23*, 4098–4107 DOI: 10.1021/ma00220a012.
- (30) Hird, B.; Eisenberg, a. Sizes and stabilities of multiplets and clusters in carboxylated and sulfonated styrene ionomers. *Macromolecules* **1992**, *25*, 6466–6474 DOI: 10.1021/ma00050a013.

- (31) Navratil, M.; Eisenberg, a. Ion Clustering and Viscoelastic Relaxation in Styrene-Based Ionomers . III . Effect of Counterions , Carboxylic Groups , and Plasticizers. *Macromolecules* **1972**, *4*, 84–89 DOI: 10.1021/ma60034a027.
- (32) Malmierca, M. A.; González-Jiménez, A.; Mora-Barrantes, I.; Posadas, P.; Rodríguez, A.; Ibarra, L.; Nogales, A.; Saalwächter, K.; Valentín, J. L. Characterization of Network Structure and Chain Dynamics of Elastomeric Ionomers by Means of ^1H Low-Field NMR. *Macromolecules* **2014**, *47*, 5655–5667 DOI: 10.1021/ma501208g.